

Cosmic magnetic fields and HE particles

Philipp Kronberg

*Los Alamos National Laboratory
and
University of Toronto*

Université libre de Bruxelles

26th November 2010



Galaxies with strong starburst-driven outflows

2 examples:



A

NGC 4569 4.85 GHz Total power + Pol. int. B-vectors

13 18

16
A&A 347,465, 2006

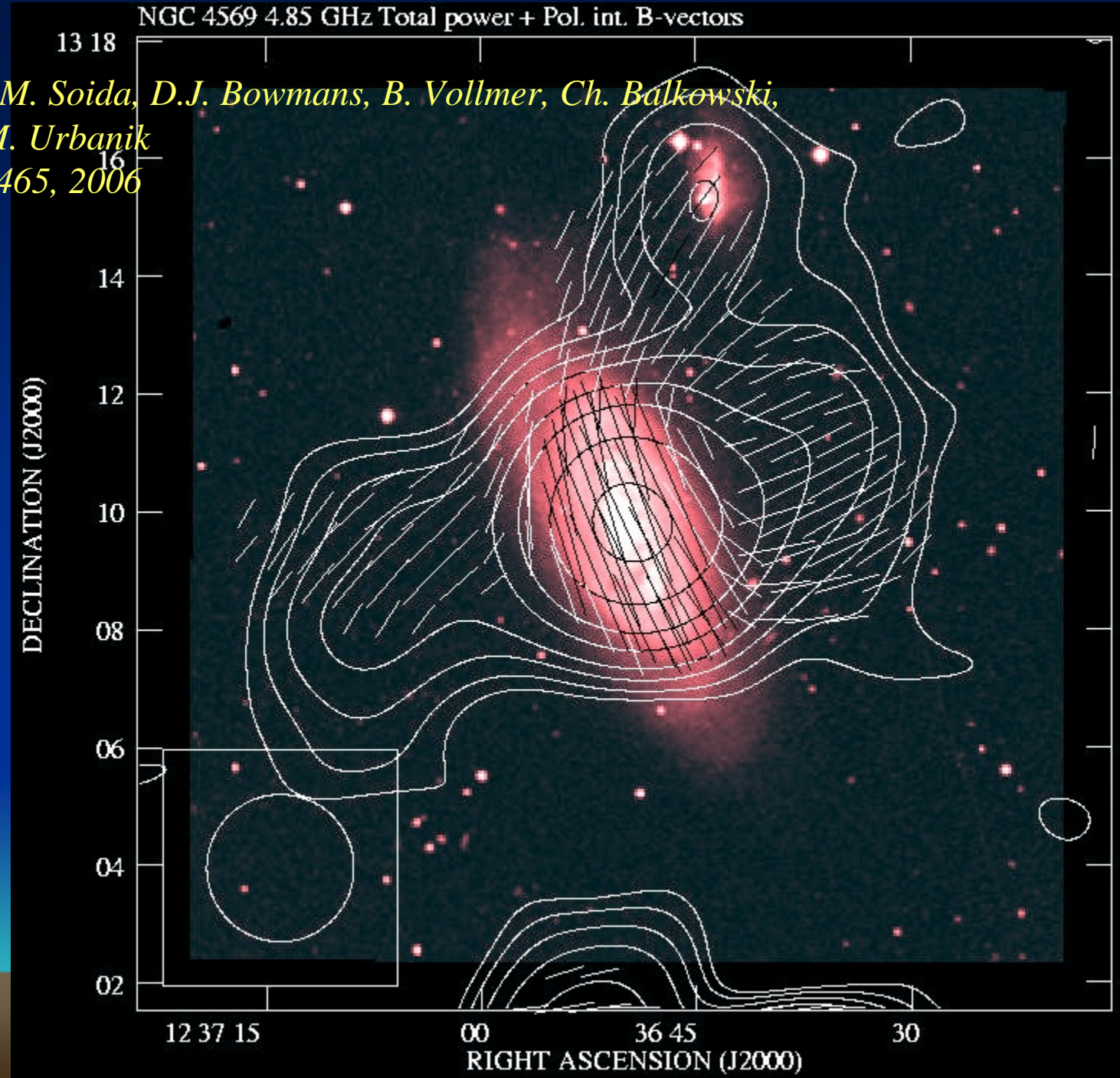
DECLINATION (J2000)

14
12
08
06
04
02

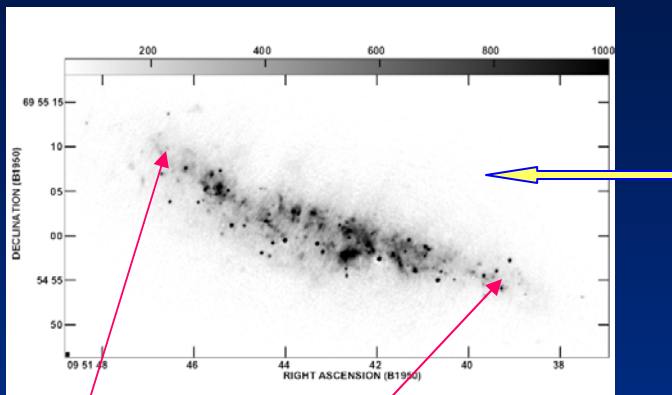
12 37 15

00 36 45 30

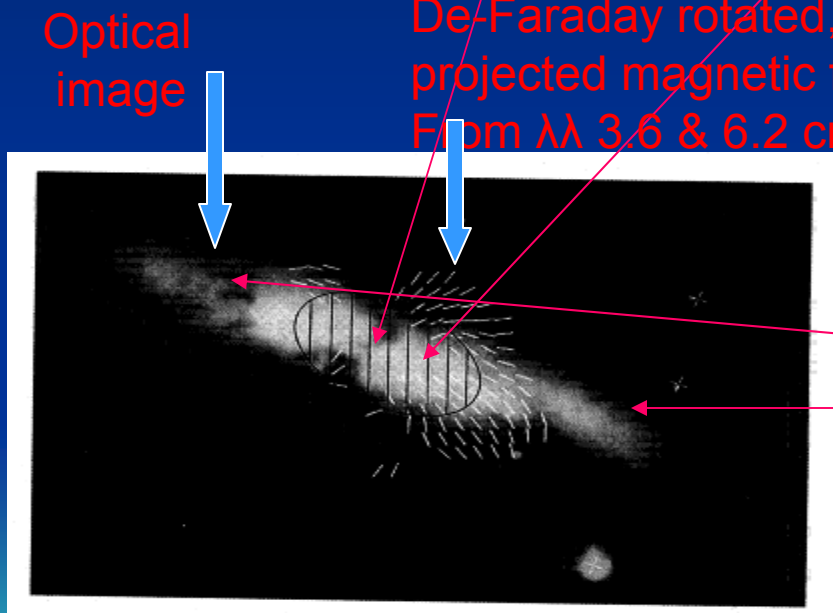
RIGHT ASCENSION (J2000)



B. Outflow from the M82 starburst galaxy (3 Mpc distant)

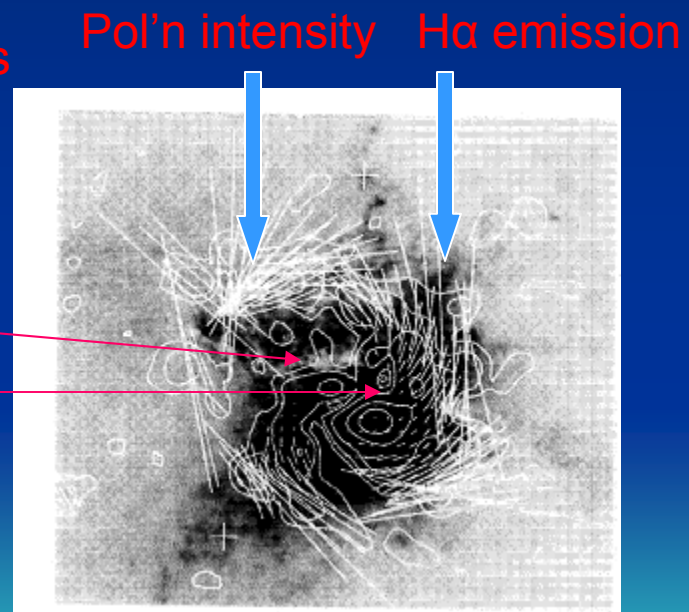


Kronberg, P.P. Biermann, P.L.
Schwab, F.R.
ApJ 246, 751, 1981.
VLA, 5 GHz, 0.3" resolution
M.L. Allen, Ph.D. Thesis 8GHz



Optical image
De-Faraday rotated,
projected magnetic field lines

From $\lambda\lambda$ 3.6 & 6.2 cm



Reuter, H.-P., Klein, U., Lesch, H., Wielebinski, R., and Kronberg, P.P. *A&A, 282, 724,*
[A&A 293, 287, 1995 - Figs. with corrected orientation].

Massive spiral galaxies
more like the Milky Way

an edge-on view:

Example of NGC891 with its projected
halo magnetic field structure



a top (plan) view



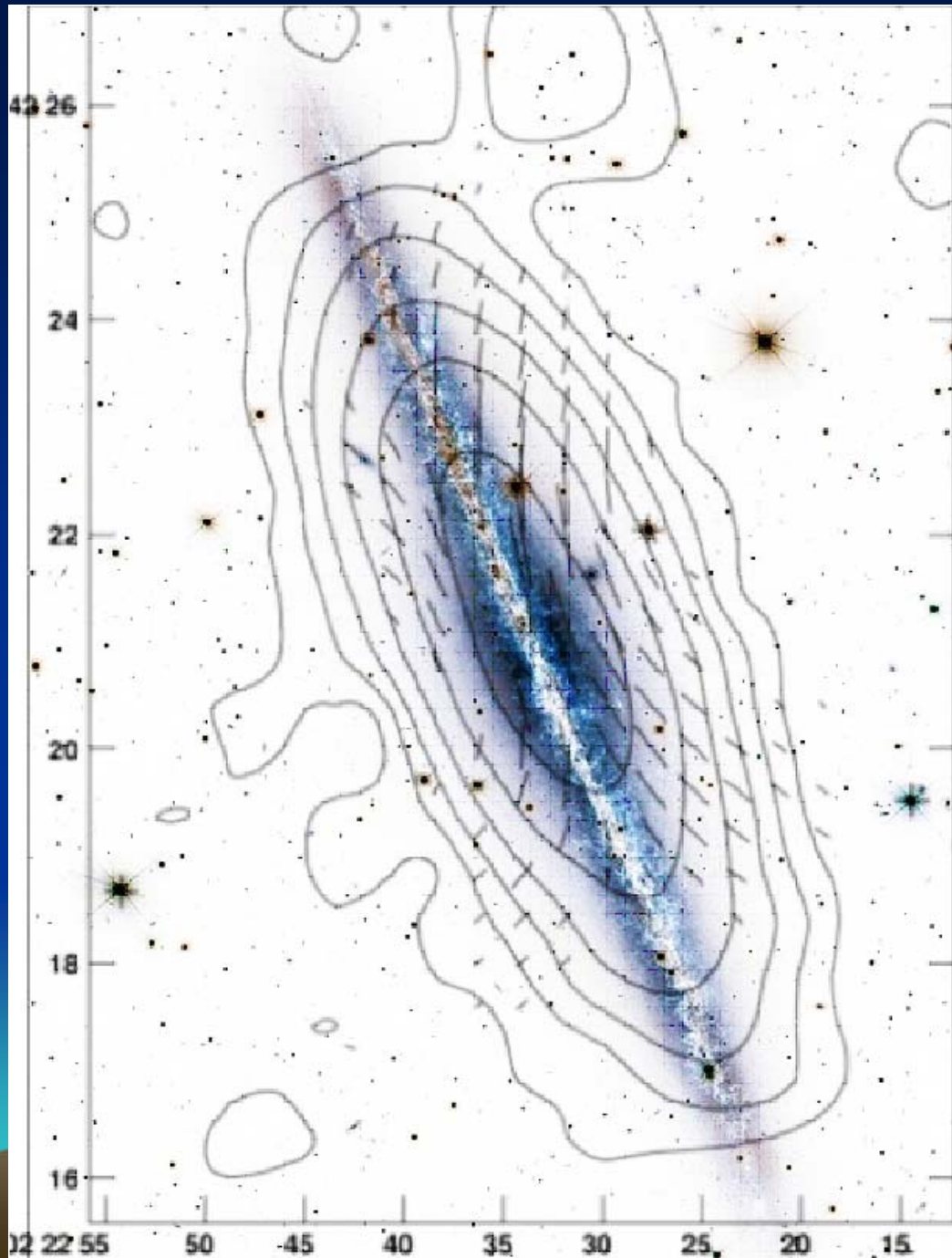
Projected Magnetic field
In a “grand design” galaxy

M51

*R. Beck
in
Sterne und Weltraum,
September 2006.*

Question: To an extragalactic observer, does the Milky Way present a clear and beautiful magnetic grand design, like M51 and others?

New results suggest yes



NGC891
Similar to the Milky Way

Edge-on view

of the (projected)
Halo magnetic field structure

So far, difficult to obtain a similar,
and 3-D halo magnetic field model
for the Milky Way

Image by M. Krause

1

A return to the Milky Way

Begin with Simard-Normandin & Kronberg

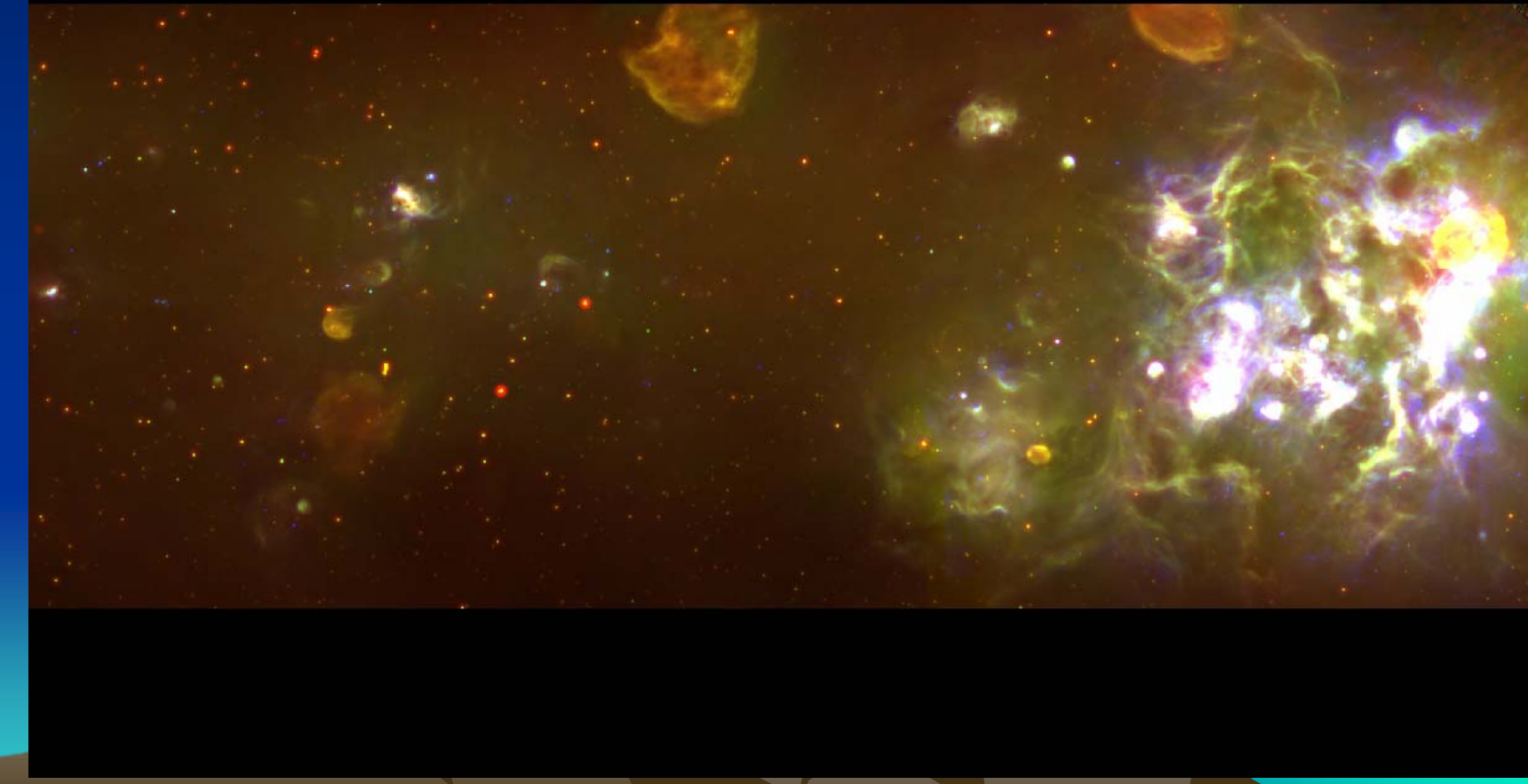
Nature **279**, 115, 1979, *ApJ* **242**, 74, 1980



Inside the plane of the Milky way disk:

a view between $b \pm 4^\circ$

A segment of the Canadian Galactic Plane survey (CGPS) at 1.4 GHz



Faraday Rotation measure studies of the Milky

“New Large Scale Magnetic Features of the Milky Way”

Simard-Normandin & Kronberg, *Nature*, 279, 115, 1979.

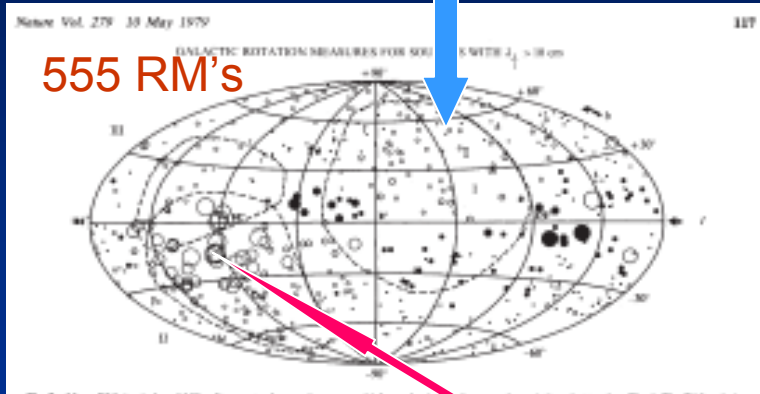


Fig. 3. Mean RM in units of 10¹⁷ rad s⁻¹ cm⁻³ for sources which complete the large-scale variations better than Fig. 1. The RM scale is the same as that of Fig. 1. The positions of the radio-contamination loops II, III and IV are marked. More obscure small-scale features which are not smoothed out, and the precise location of boundaries where the RM change sign are not easily stated. These are best located in Fig. 1.

The large scale of feature A (implied by its large RM) requires that it have a large magnetic energy, $\approx 10^{11}$ erg. On this consideration alone, RM feature A is too energetic to be associated with a supernova remnant. On energetic grounds it could be associated with either galactic rotation or large-scale streaming of the infalling high-velocity HI clouds, of which there are several in the same direction^{1,2,3}. It is possible that feature A is associated with local streaming effects which are related to the magellanic streams, because the end of the magellanic stream lies in the approximate direction of feature A. More data are required, however, to establish any connection with the magellanic streams.

The structure of magnetic field

The large rotation measures observed near the galactic plane around $l=235^{\circ}$ (feature B) and $l=90^{\circ}$ are consistent with a longitudinal magnetic field directed towards $l=90^{\circ}$. In the direction opposite to galactic rotation the large RM area is centred near 255° rather than 210° which suggests that the Perseus arm may be passing up in this direction. The RM and dispersion measures (DM) of pulsars in this direction indicate a mean magnetic field of less than 3 µG (90° and 270° south of the galactic plane). From this we conclude that the extent of the aligned field in both these areas (A and B) is greater than ~ 4 kpc. A and B must therefore be large-scale features of the Galaxy. Feature C at $l=45^{\circ}$ can be interpreted as another major longitudinal component located approximately between the Sagittarius and the Norma-Sextans arm where the magnitude of the RM suggests the prevailing field is directed along our line of sight for several kiloparsecs.

The very abrupt reversal of RM near the plane at $l=60^{\circ}$ is consistent with a model containing two prevailing field axes pointing in opposite directions along the spiral interarms. This is best shown in Fig. 5, in which we superimpose the model of the spiral structure of the Galaxy by Gosseline¹.

The fields do not seem to be co-planar. They also extend to quite large angular distances from the main galactic plane. An interesting question at this stage is whether a remnant—let us say, region C—can be seen on the $J < 360^{\circ}$ side of the Galaxy—in the southern hemisphere. Unfortunately, we have not made

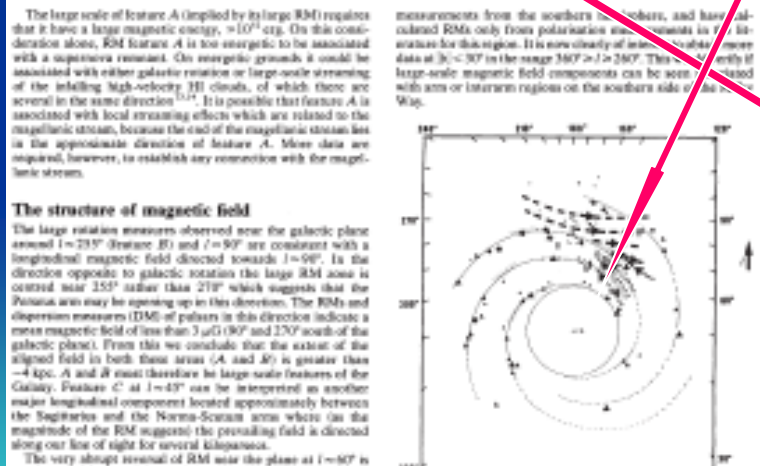


Fig. 4. A sketch of the regions containing an aligned component of magnetic field, indicating their approximate radii and directions. This is shown superimposed on the distribution of bright HII regions in the Galaxy by Gosseline¹. Note that the heavy dotted and dashed lines do not necessarily represent the local prevailing magnetic field directions, but rather the zones in which the line-of-sight integral of RM is large and has the same sense.

Summary of conclusions in 1980:

Simard-Normandin & Kronberg
ApJ 242, 74, 1980

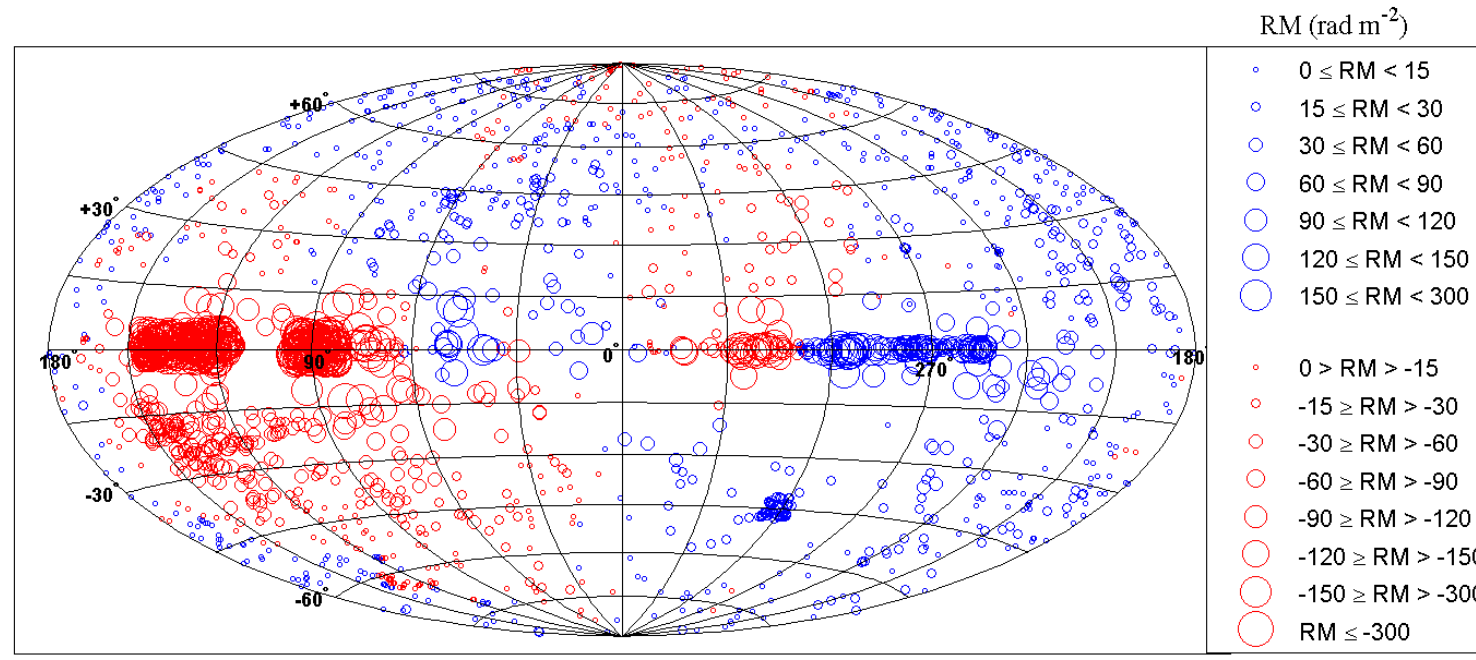
1. Bisymmetric field pattern
2. Off-plane angular autocorrelation scale of RM sign $\approx 30^{\circ}$
3. Magneto-ionic scale height ≈ 1.8 kpc
4. (Still mysterious) off-plane, high-RM zone at $l \sim 100^{\circ}$, $b \sim -25^{\circ}$ (region “A”)
5. Spiral with 15° (from tangential) pitch angle



Updated RM probe of the Milky Way disk

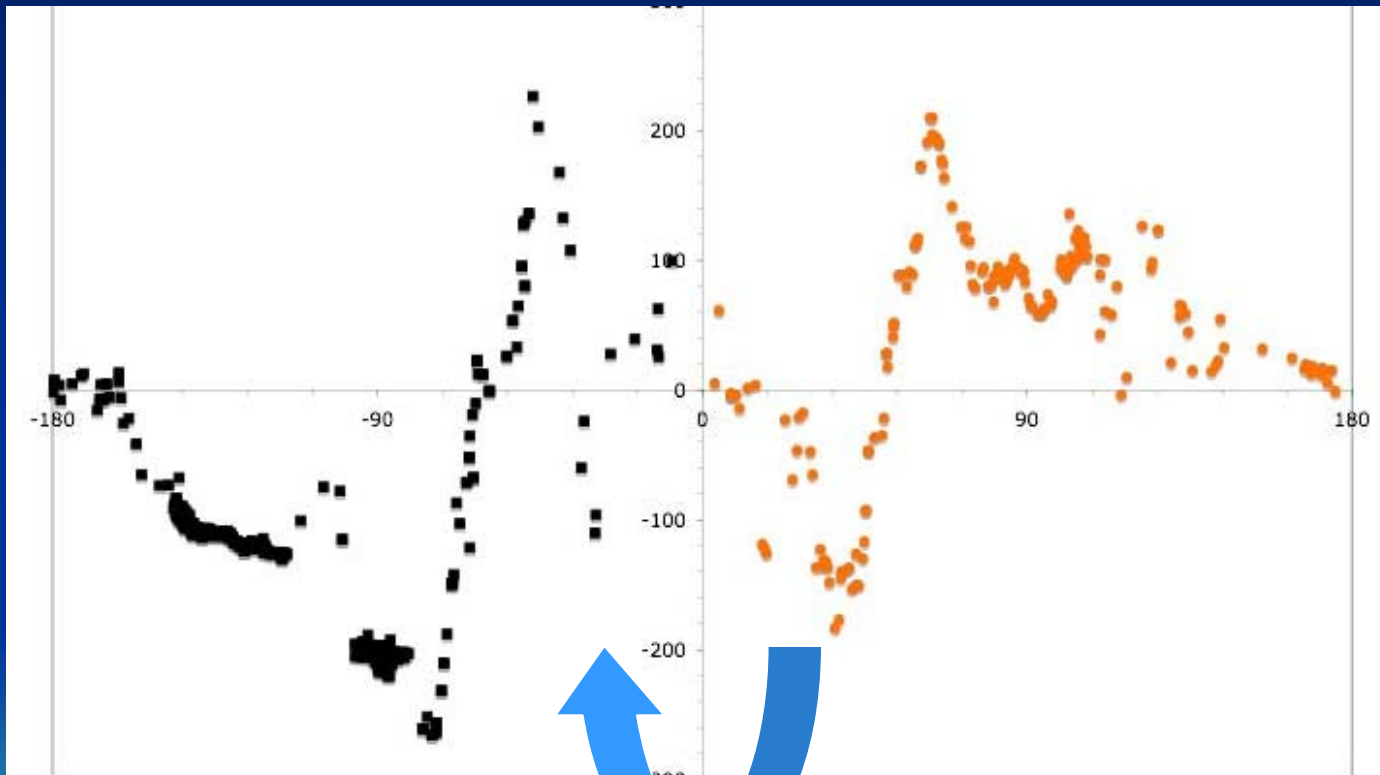
New evidence

New smoothed Galactic RM sky from 2250 egrs RM's



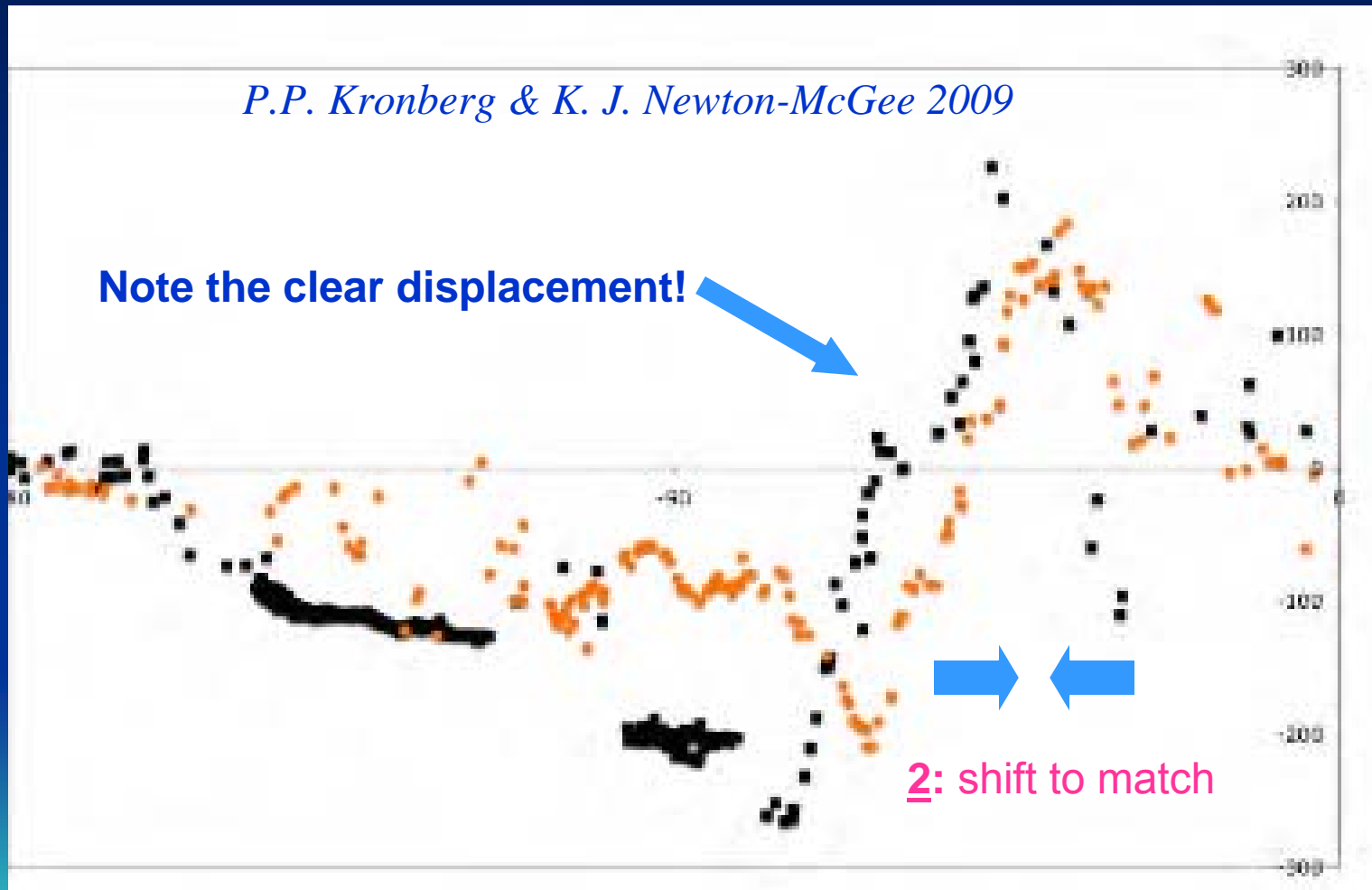
Smoothed RM's around the Galactic plane at $|b| \leq 10^\circ$ *New evidence for $\langle B \rangle$ in the disk*

P.P. Kronberg & K. J. Newton-McGee arXiv:0909.4753



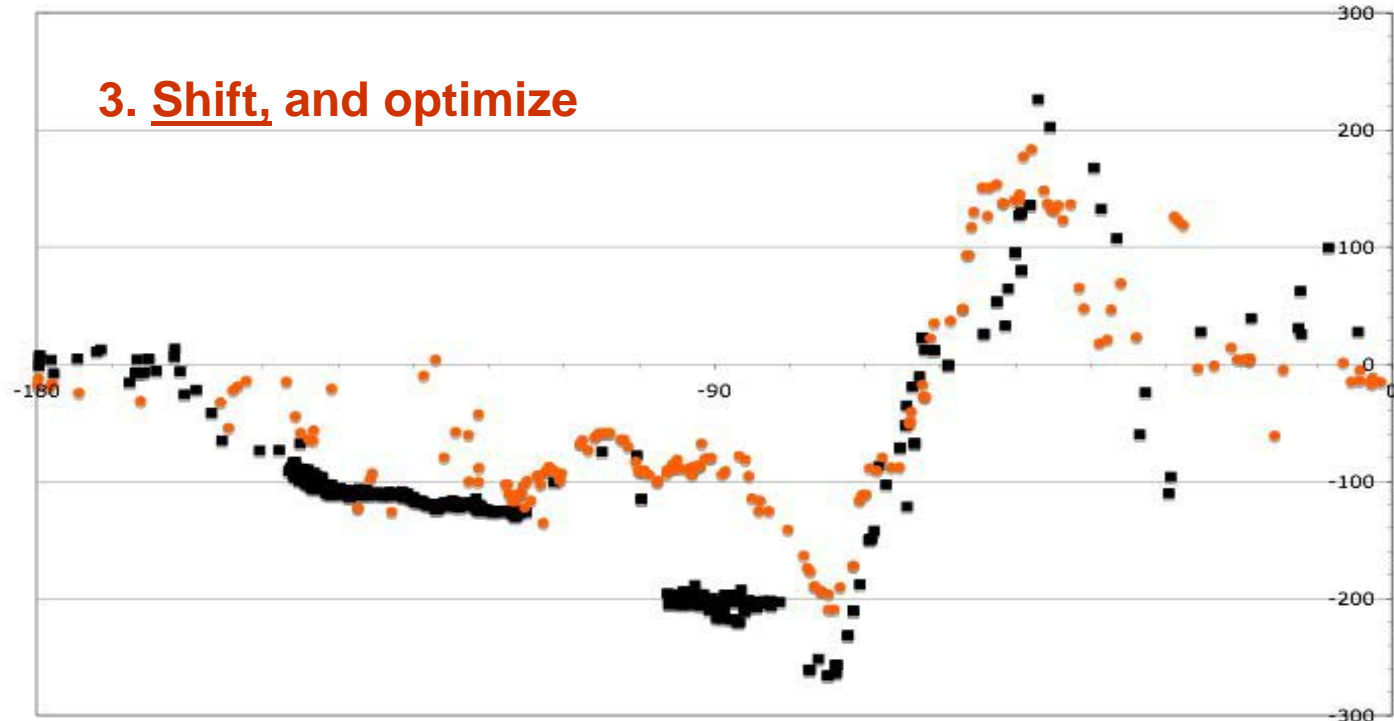
1. fold about the Galactic center direction ($l=0^\circ$),
and reverse sign

Fold RM's about $l=0$, then **reverse the sign**
of RM's at $360^\circ > l > 180^\circ$ (orange points)

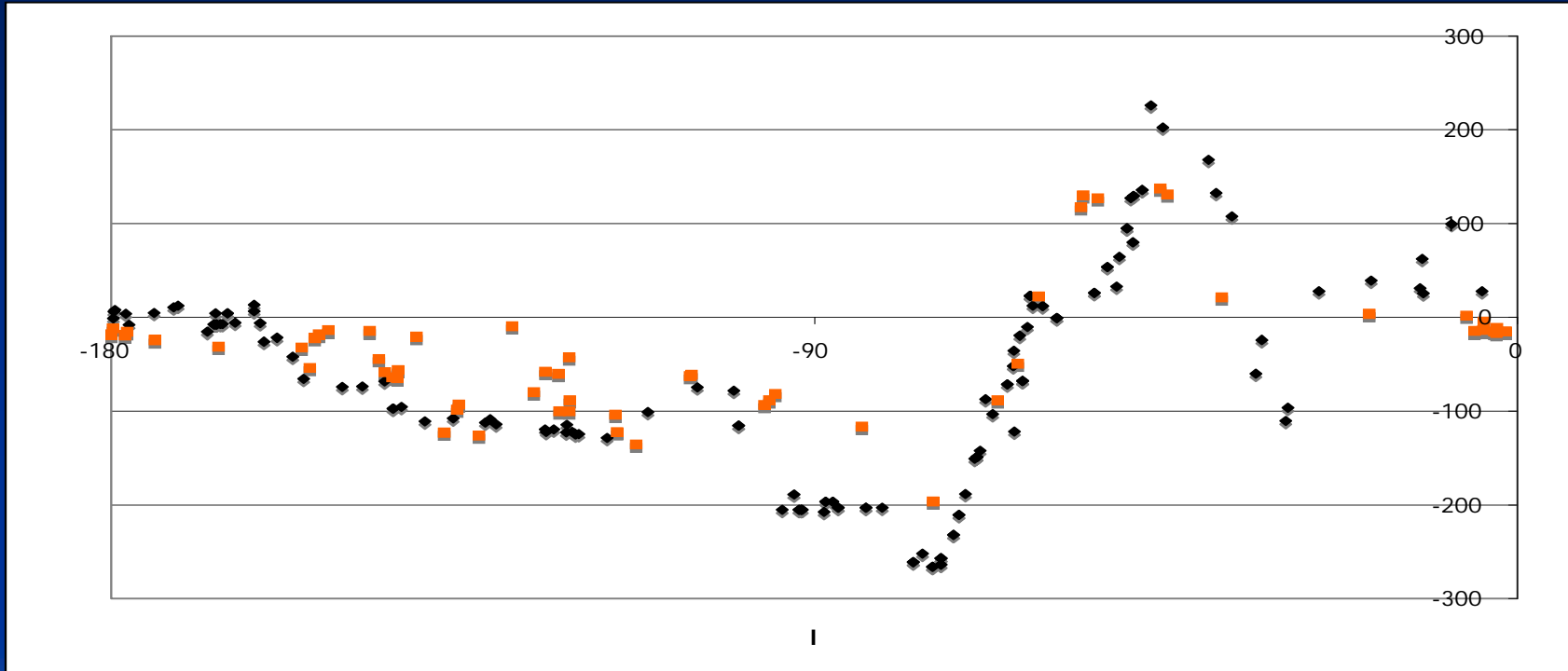


RM's *after* an 11° ($\pm 2^\circ$) shift

3. Shift, and optimize



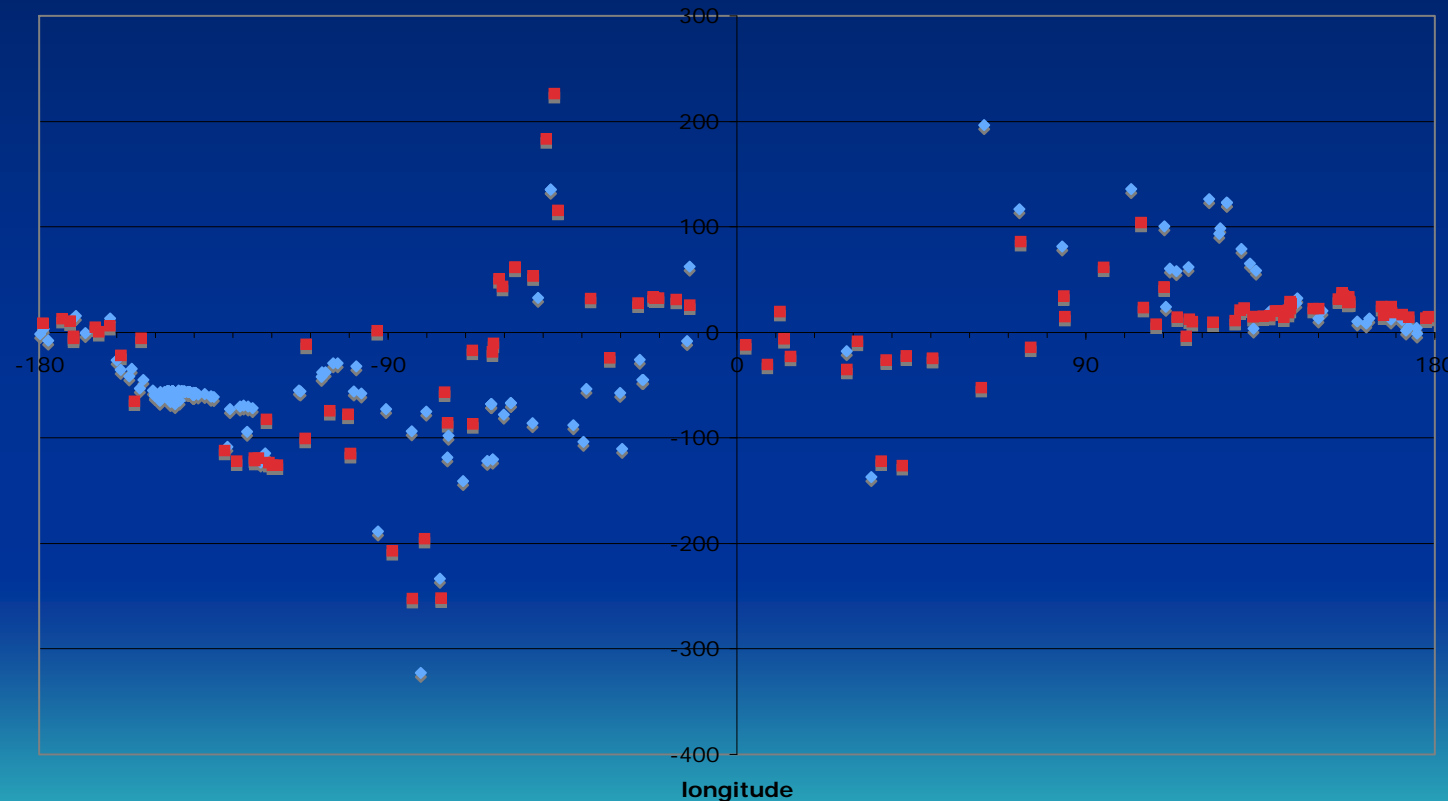
Smoothed RM's up to $b = |10^\circ|$ CGPS and SGPS omitted RM's folded and 11° -shifted, as before



Conclusion:
 $\langle \text{RM} \rangle$ at $|b| \lesssim 2^\circ$ is coupled to $\langle \text{RM} \rangle$ at $(2^\circ \lesssim |b| \lesssim 11^\circ)$, at \sim all I

This pattern deteriorates only at $|b| \gtrsim 12^\circ$ -- see next

Now, migrate further away from the Galactic plane

$$5^\circ < |b| < 20^\circ$$


Quick summary of results

1. Our RM smoothing resolution is comparable with (1) the galactic z -height (~ 1.5 kpc), and (2) inter-arm spacing ($\sim 1 - 2$ kpc). It averages over smaller-scale B reversals.
2. Spiral pitch angle is $11 \pm 2^\circ$. (This can be confirmed only on our side of MW disk). Similar to recent Han et al RM result, and Heiles (1996) based on interstellar polarization data.
3. Average B aligns closely with the stellar spiral structure –like many other nearby spirals
4. To an extragalactic observer, the magnetic Milky Way is a highly patterned, “grand design” spiral galaxy, just like M51, etc.!! – **when we look at the forest, not the trees!!**
5. Major sign reversal occurs near $l = 55^\circ$ – consistent with a bisymmetric “BSS” pattern. **ASS outer** structure. BUT recall that we “see” only our side of the Milky Way disk

B in the galactic Halo?

*Mao , S.A., Gaensler, B. M., Haverkorn, M., Zweibel, E.G.,
Madsen, G. J., McClure-Griffiths, N. M., Shukurov, A.,
Kronberg, P. P. ApJ **714**, 1170, 2010*

In the NGH: median RM = 0 ± 0.5 rad/m²

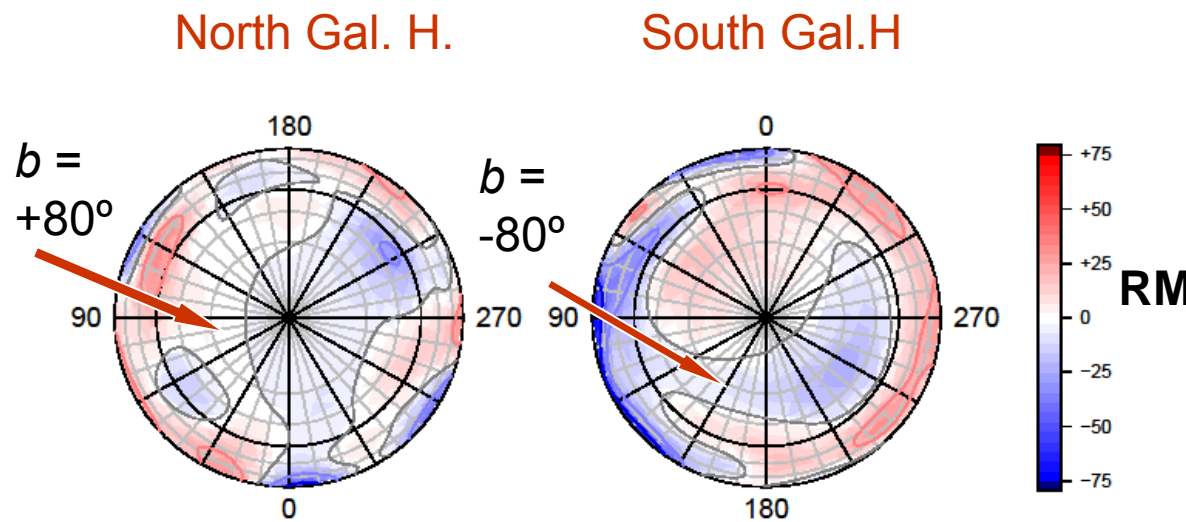
In the SGH: medium RM = $+6.3 \pm 0.7$ rad/m²

$\sigma = 9$ rad/m² indep. of angular scale up to 25° -> $\sigma_B \sim 1 \mu G$



Bayesian smoothed RM's in the Galactic caps $|b|>30^\circ$

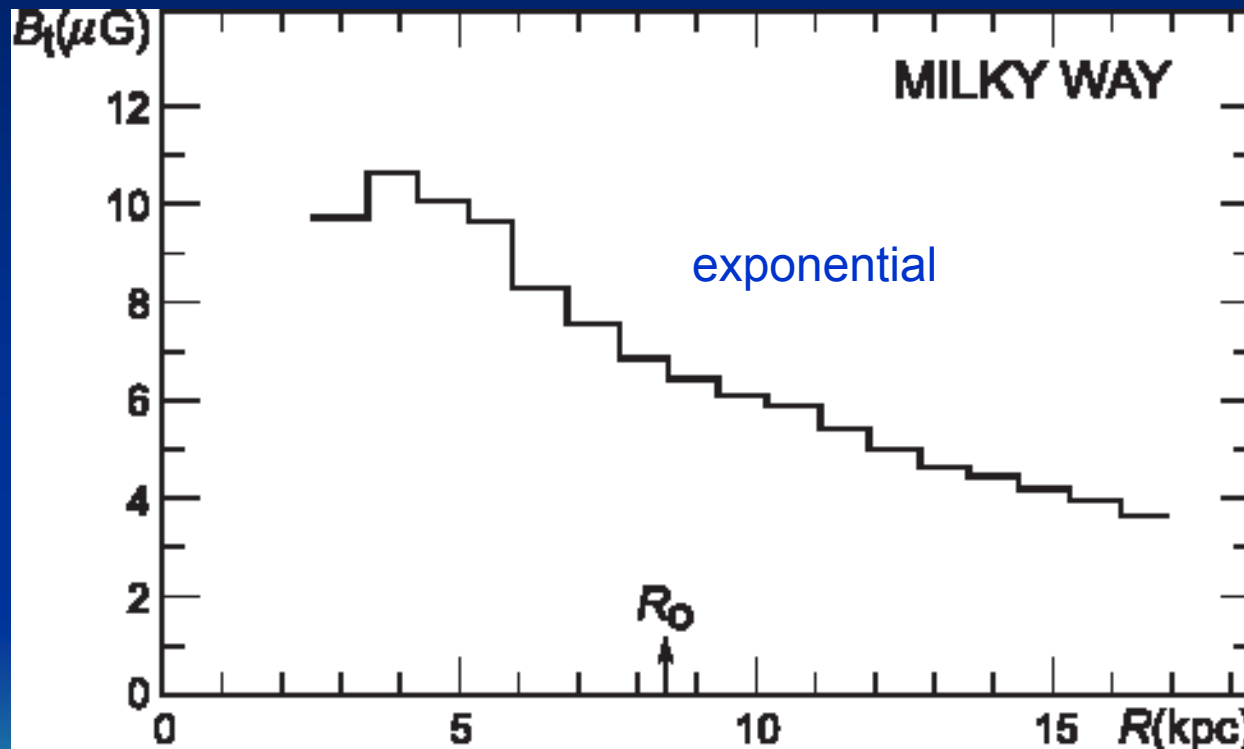
M.B. Short, D.M. Higdon & P.P. Kronberg
Bayesian Analysis 2, 665, 2007



Better data and more refined analysis are underway

$|B| (R)$ in the Milky Way disk.

Galactic disk field $\langle |B| \rangle$ vs R , modelled from all-sky continuum radiation at 0.4GHz (Haslam *et al.*) and 1.4 GHz (Reich et al.)



(E.M Berkhuijsen, W. Reich 2005, 2009)

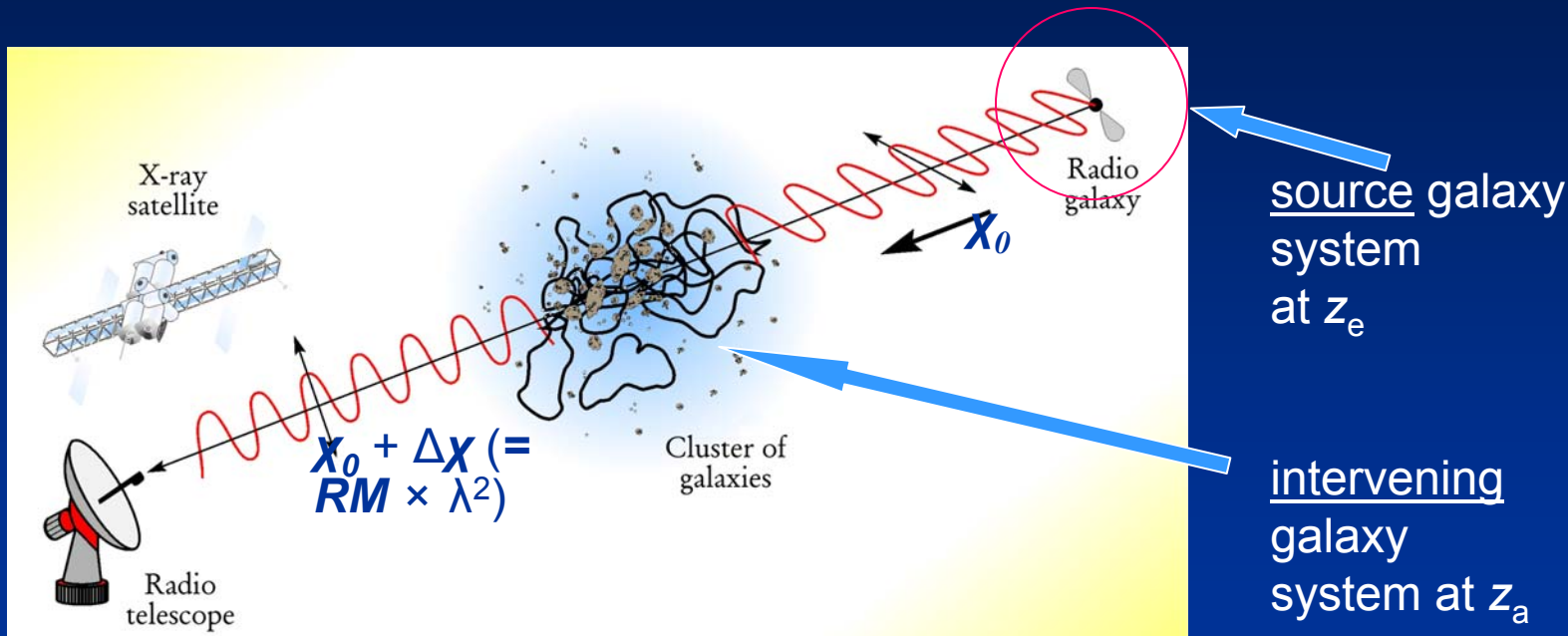
2.

NEARBY EXTRAGALACTIC SPACE
Observations, theory and modelling for
extragalactic B – fields in the
nearby ($\lesssim 150$ Mpc) universe

-- relevant to UHECR propagation



Faraday rotation at a distant EGRS, and at an interloper

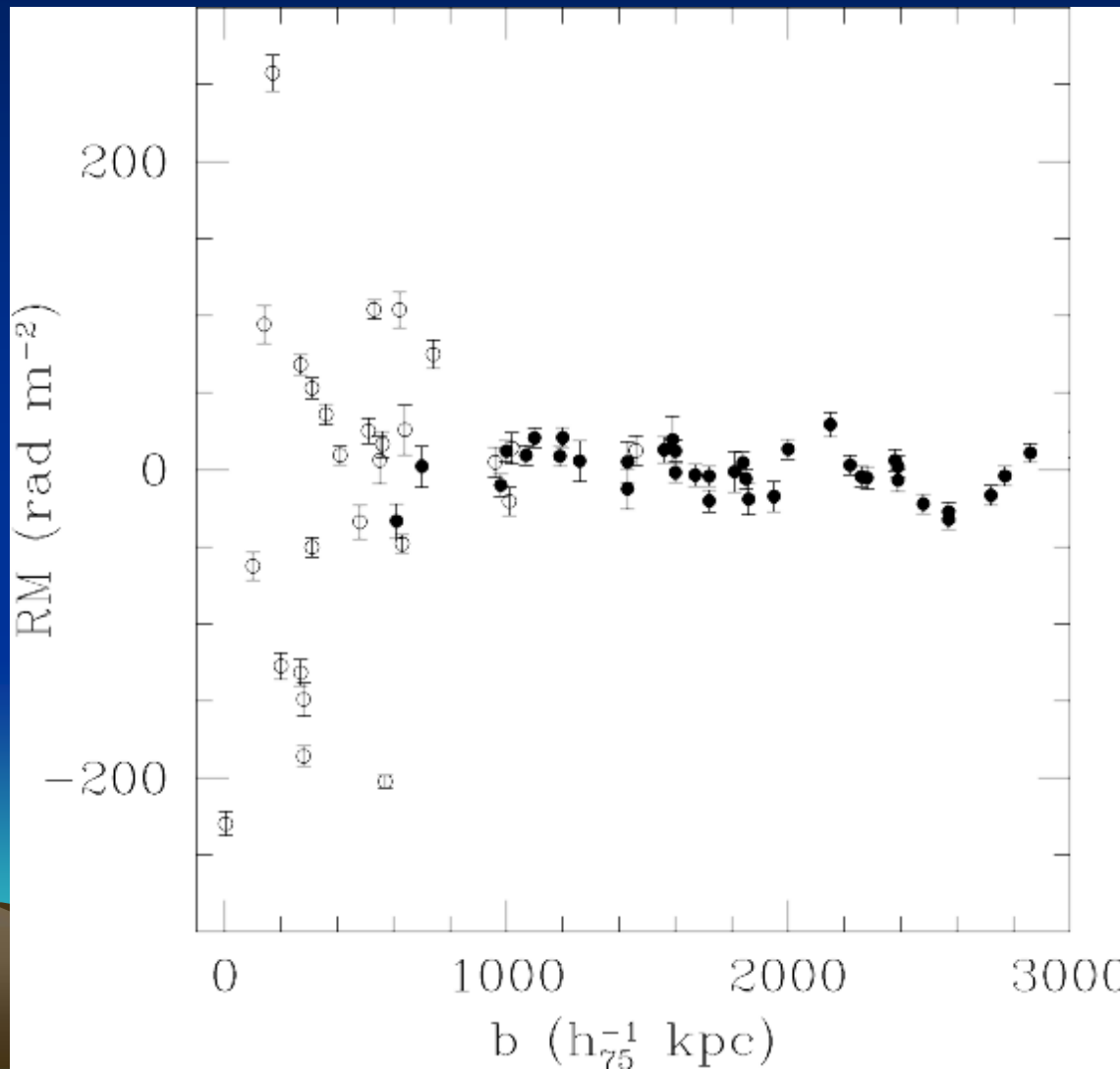


$$RM = \frac{\Delta\chi}{\Delta\lambda^2} = 8.12 \times 10^5 \int_0^{z_s} (1+z)^{-2} n_e(z) B_{||}(z) dl(z) \text{ rad m}^{-2}$$

B in Gauss, n_e in cm^{-3} , l in pc

RM of radio sources within, behind, and behind/beside, a sample of (ROSAT X-ray-selected) **galaxy clusters**

Plotted against impact parameter to the cluster center
Clarke, Kronberg, & Böhringer ApJL 547, 111, 2001



cluster redshifts are typically < 0.2

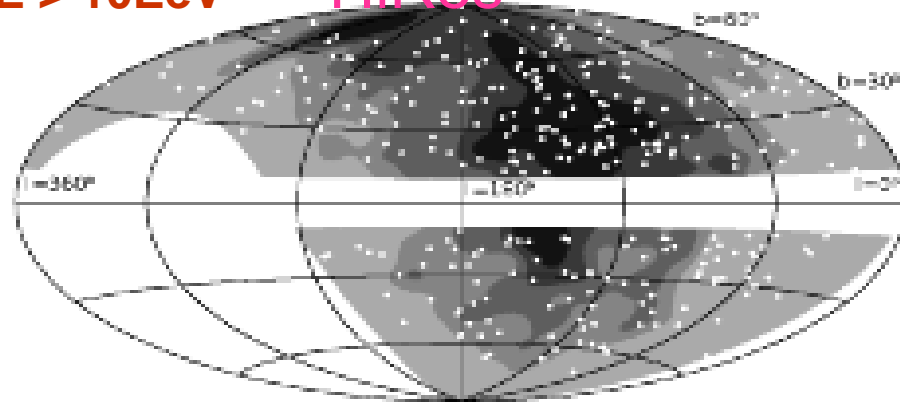
P.P. Kronberg

UHECR ANISOTROPIES(?)

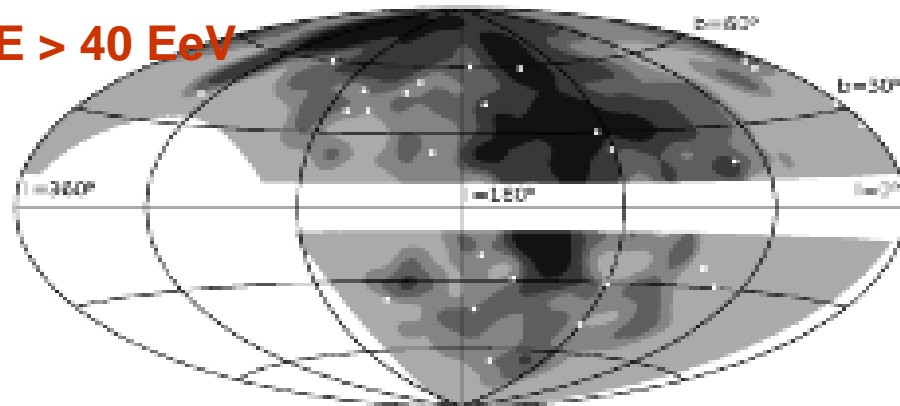


$E > 10\text{EeV}$

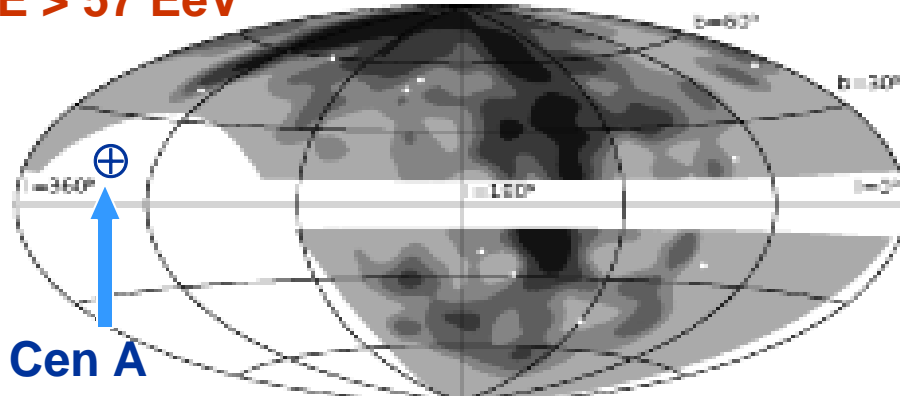
HiRes



$E > 40\text{ EeV}$



$E > 57\text{ EeV}$



Abbasi et al. arXiv:1002.1444
ApJL 2010

2(a). “Analysis of large scale anisotropy of UHECR’s in HiRes data”

Grey scale steps display

$$\Phi = \Phi \cdot \Xi$$

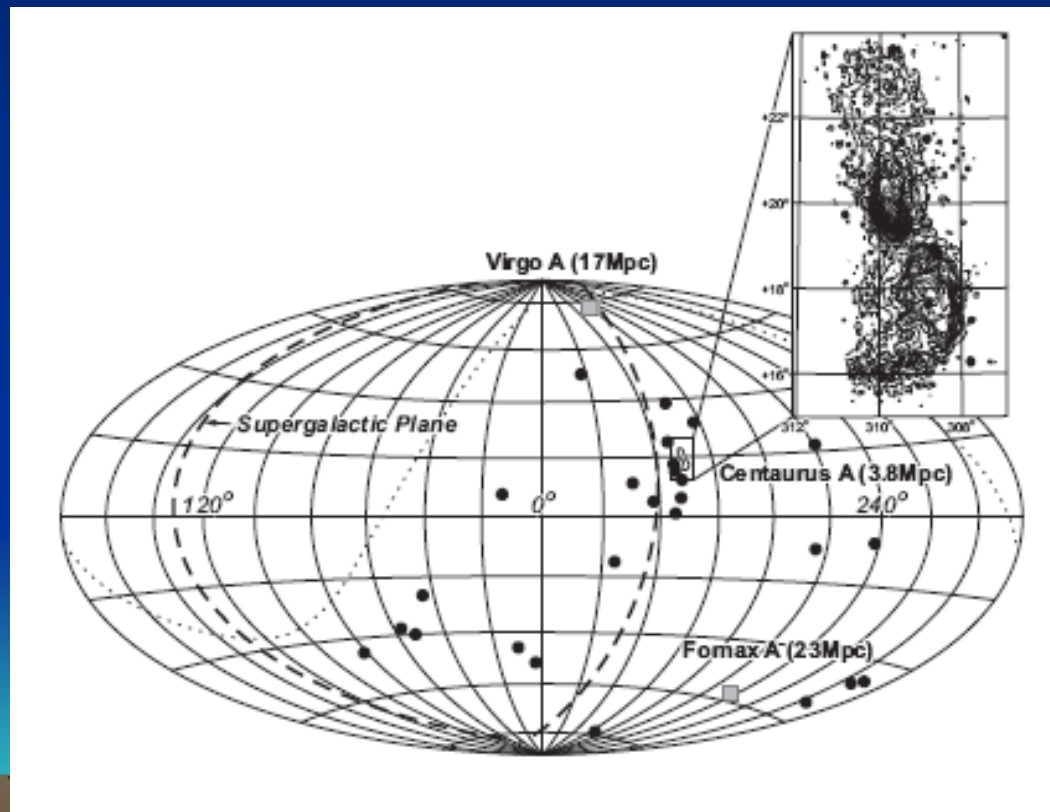


Exposure
function

model mass distr.
function
(with 9° smeering)

2(b) Case of Centaurus A at 3.8 Mpc 27 events above 6×10^{19} eV detected by the Auger collaboration

UHECR events: The Pierre Auger Collaboration, Science, 318, 938, 2007



Cent A image: N. Junkes et al. A&A, 269, 29, 2003/Patricia Reich (priv. comm.)

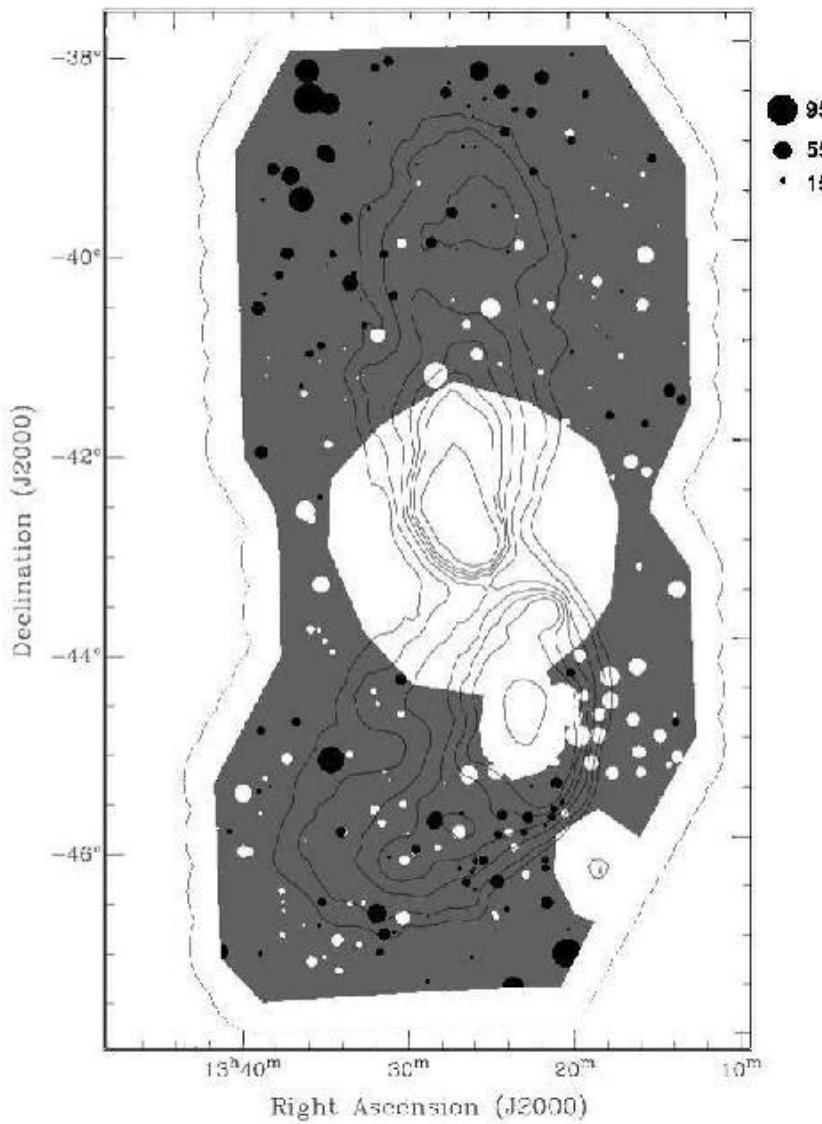


FIG. 7.— Locations and RMs of the 281 sources in Table 3. To better highlight the variations, the diameter of the sources represent the amplitude of their residual RM after the mean RM of the whole distribution (-57 rad m^{-2}) has been subtracted. Black and white sources are those with positive and negative residuals from the mean, respectively. Overlaid are Parkes 1.4 GHz radio continuum contours of Centaurus A. Contour levels are 1.5, 2, 3, 4, 5, 6, 10, 100 Jy beam⁻¹. The legend on the right hand side of the figure shows the relation between the source diameter and the absolute value of the mean-subtracted RM in units of rad m^{-2} .

Faraday Rotation measures around, and behind the Centaurus A radio galaxy (3.8Mpc distance)

Feain, I., J. Ekers, R.D.,
Murphy, T., Gaensler, B.M.,
Marquart, J-P, Norris, R.P.,
Cornwell, T.J., Johnson-Hollitt, M.,
J. Ott, & Middelberg, E.

ApJ 707, 114, 2009

Deflection of UHE CR trajectories through the magnetic environment of the local universe

$$\theta \approx 8^\circ Z \left(\frac{l}{10 \text{ Mpc}} \right)^{0.5} \left(\frac{l_0}{1 \text{ Mpc}} \right)^{0.5} \left(\frac{E}{10^{20} \text{ eV}} \right)^{-1} \left(\frac{B}{10^{-8} \text{ G}} \right)$$

Sample calculation relevant to Centaurus A ($l_0 < l$):

For protons ($Z = 1$), $l = 4 \text{ Mpc}$, $l_0 = 1 \text{ kpc}$, $E = 10^{20} \text{ eV}$, $B = 10^{-7} \text{ G}$

$$\theta = 4.8^\circ$$

How do magnetic fields get into the intergalactic medium?



3(a).

The magnetic energy input from central BH's
to the IGM

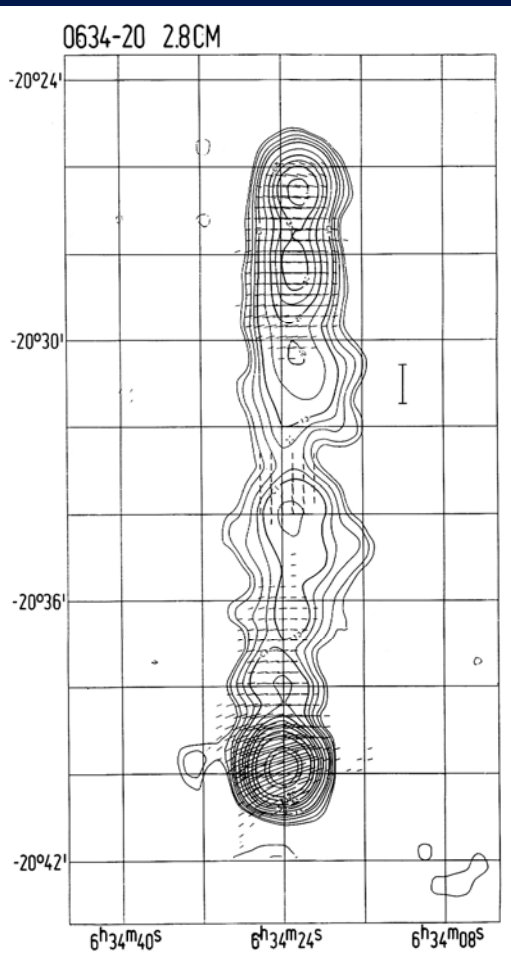
*Relevant to B in galaxy-overdense
cosmic filaments*



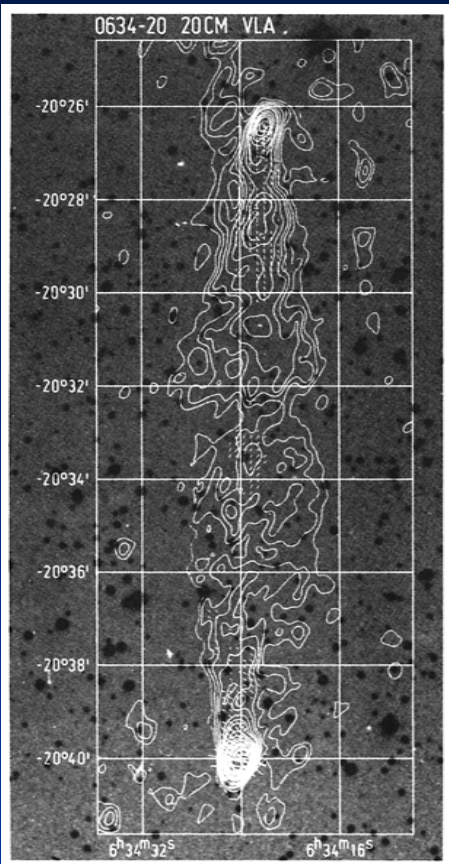


Fig. 8. The distribution of rotation measure over 3C 326 as computed from the 49 cm and 21 cm convolved data superposed upon a “photograph” of the 49 cm total intensity. Note that to produce a simple grid of single digit numbers we have subtracted integrated rotation measures, whose derivation is described in the text, of $+25 \text{ rad m}^{-2}$ and $+20 \text{ rad m}^{-2}$ from the values measured at individual sample points in the east and west components respectively. For reference, these integrated values are displayed under each component

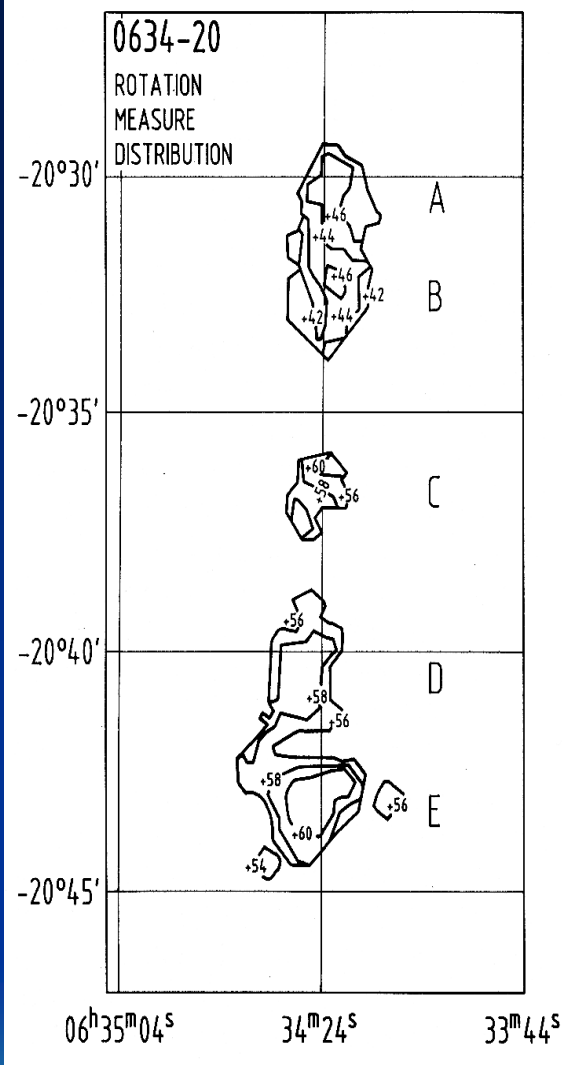
10 GHz



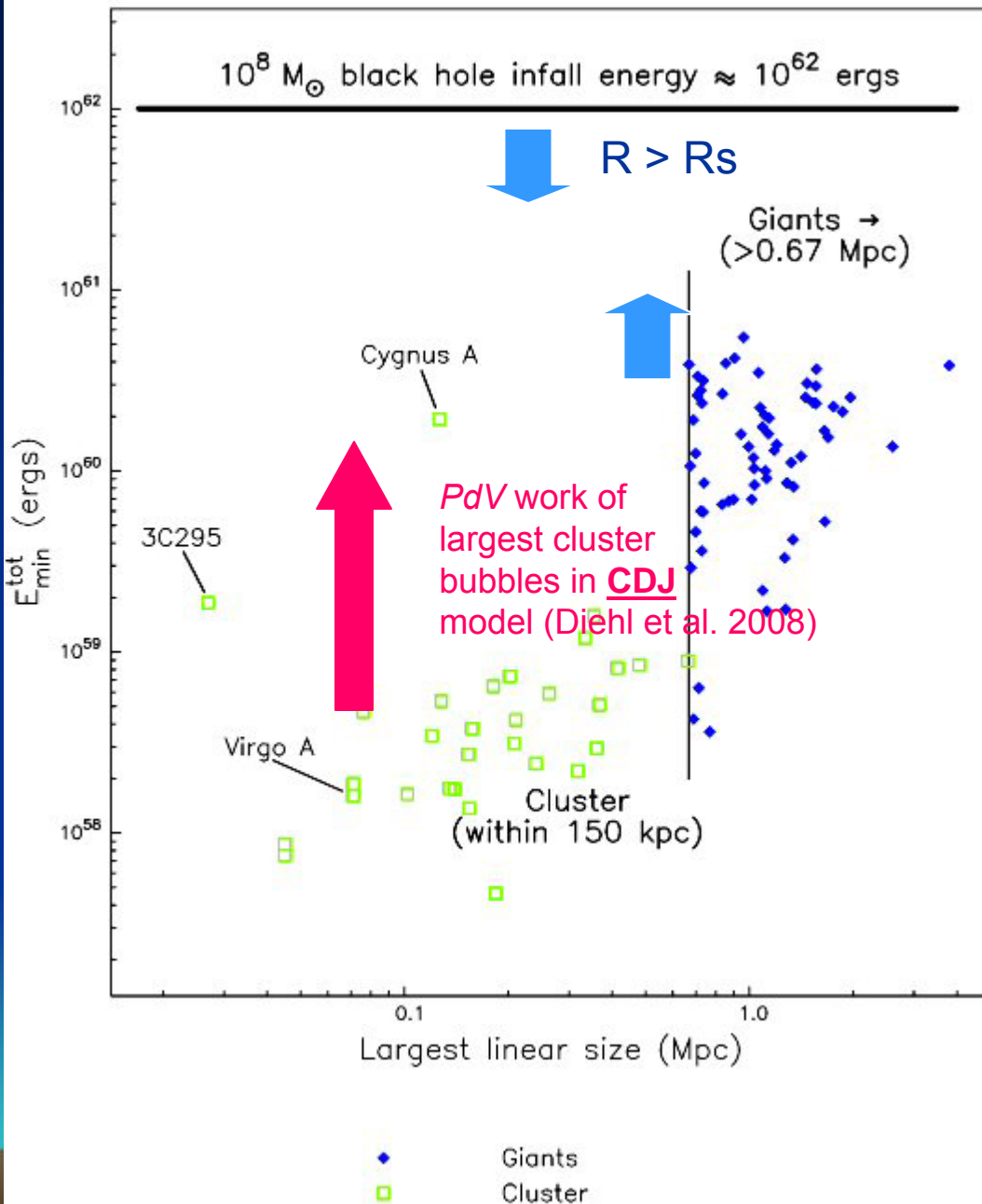
1.4 GHz



Faraday RM(radians/m²)



Kronberg, Wielebinski & Graham
A&A 169, 63, 1986



$$= M_{\text{BH}} C^2$$

Mind the gap!!

Accumulated energy
 $(B^2/8\pi + \varepsilon_{\text{CR}}) \times (\text{volume})$
 from ``mature'' BH-powered
 radio source lobes

GRG's
 capture the highest fraction
 of the magnetic energy
 released to the IGM

Kronberg, Dufton, Li, &
 Colgate,
 ApJ 560, 178, 2001

Expectation of the average intergalactic field seeded by supermassive black holes: A global calculation

Average galactic
BH density
($M_{\text{BH}} \gtrsim 10^{6.5} M_{\odot}$)

$$\langle \rho_{\text{BH}} \rangle \approx 2 \times 10^5 M_{\odot} / \text{Mpc}^3$$

Gravitational energy reservoir per BH
(scaled to infall to R_S)

$$\varepsilon_B = 1.36 \times 10^{-15} \left(\frac{\eta_B}{0.1} \right) \times \left(\frac{f_{\text{RG}}}{0.1} \right) \times \left(\frac{f_{\text{FILAMENTS}}^{\text{VOL}}}{0.1} \right)^{-1} \times \left(\frac{M_{\text{BH}}}{10^8 M_{\odot}} \right) \text{ erg cm}^{-3}$$

Gives $B_{\text{IG}}^{\text{BH}} = \sqrt{8\pi\varepsilon_B} = 1.8 \times 10^{-7} \text{ G}$

- Initially captured within galaxy filaments
- Intergalactic medium near galaxies should contain significant magnetic energy, originating in central BH's

3 (b)

- First test for $\langle |B_{\text{IGM}}| \rangle$ in nearby galaxy supercluster filaments --
- If $\langle |B_{\text{IGM}}| \rangle \approx 10^{-7}\text{G}$ on scales of few $\times 100$ kpc, it has a chance of being detectable in RM

Y. Xu et al ApJ 637, 19, 2006

LSS out to ≈ 110 Mpc

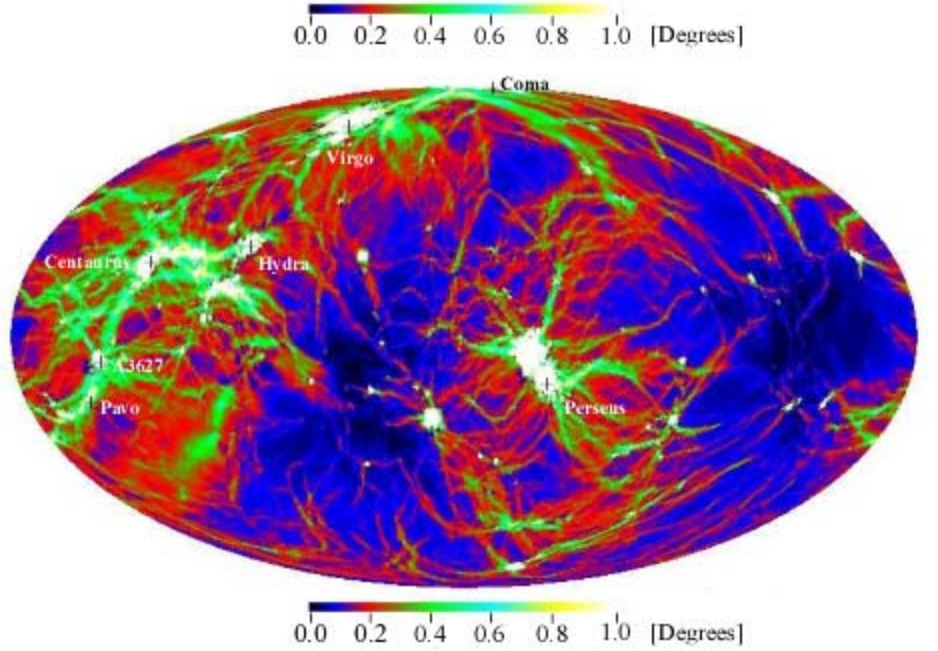
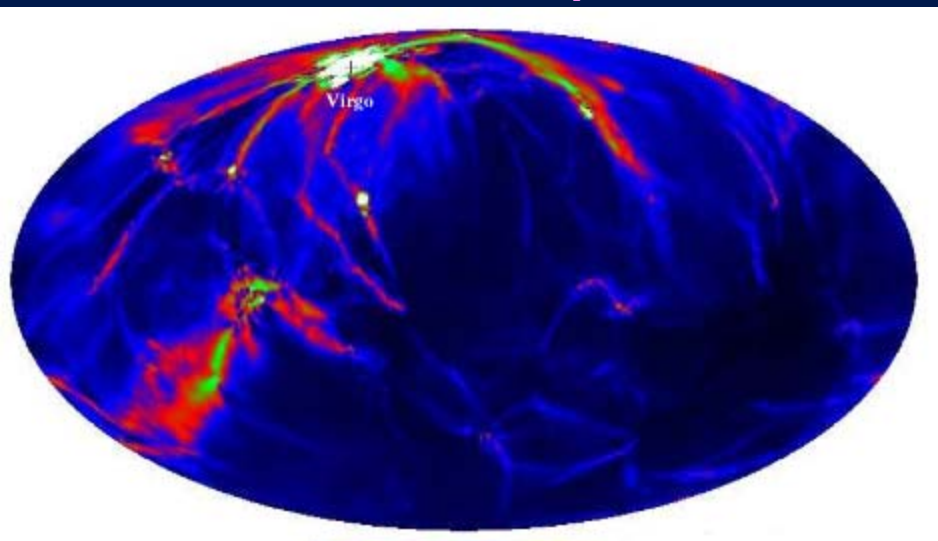


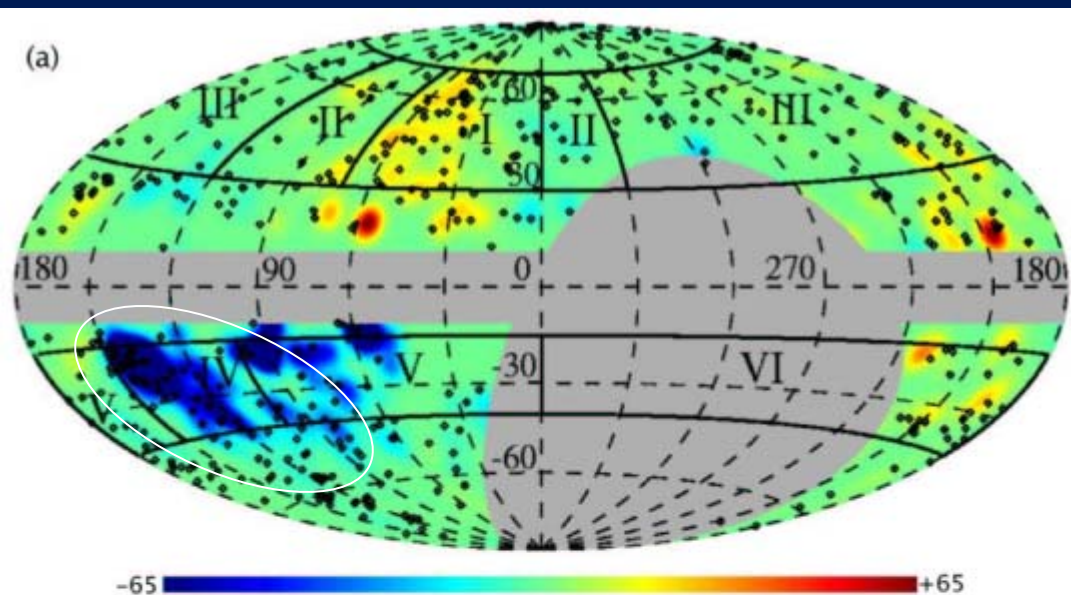
Fig. 14.— Full sky maps of expected deflection angles for protons with the arrival energy $E = 4 \times 10^{19}$ eV. The upper panel is restricted to the 25 Mpc propagation distance, while in the lower panel the whole simulation volume within a radius of 110 Mpc around the position of the Galaxy was used.

B_{IGM} in the local Universe and UHECR propagation

K. Dolag, D. Grasso, V. Springel & I. Tkachev

J. Cosm. & Astroph. Phys. 1:009, 2005

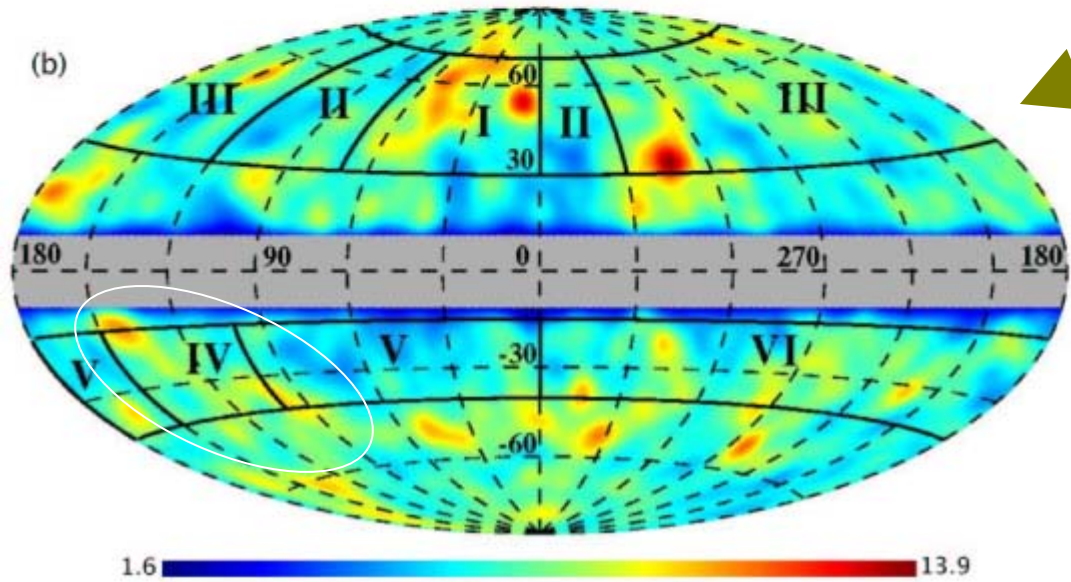
- Seed field at high redshift
- $|B|$ growth driven by LSS formation (gravity)
- MHD field amplification
- $\approx 10^{-12}$ G (voids) – few $\times 10^{-6}$ G(Clusters)



SMOOTHED
FARADAY
ROTATION

Region containing
the Perseus-Pisces
supercluster

rad/m²



GALAXY COLUMN
DENSITY
(Method #2:
2MASS survey,
HEALPix algorithm)

galaxies
per pixel
(\propto column density)

Optical galaxy counts vs. RM plots
for the Perseus-Pisces supercluster chain
Two types of investigation

Xu et al. ApJ 2006

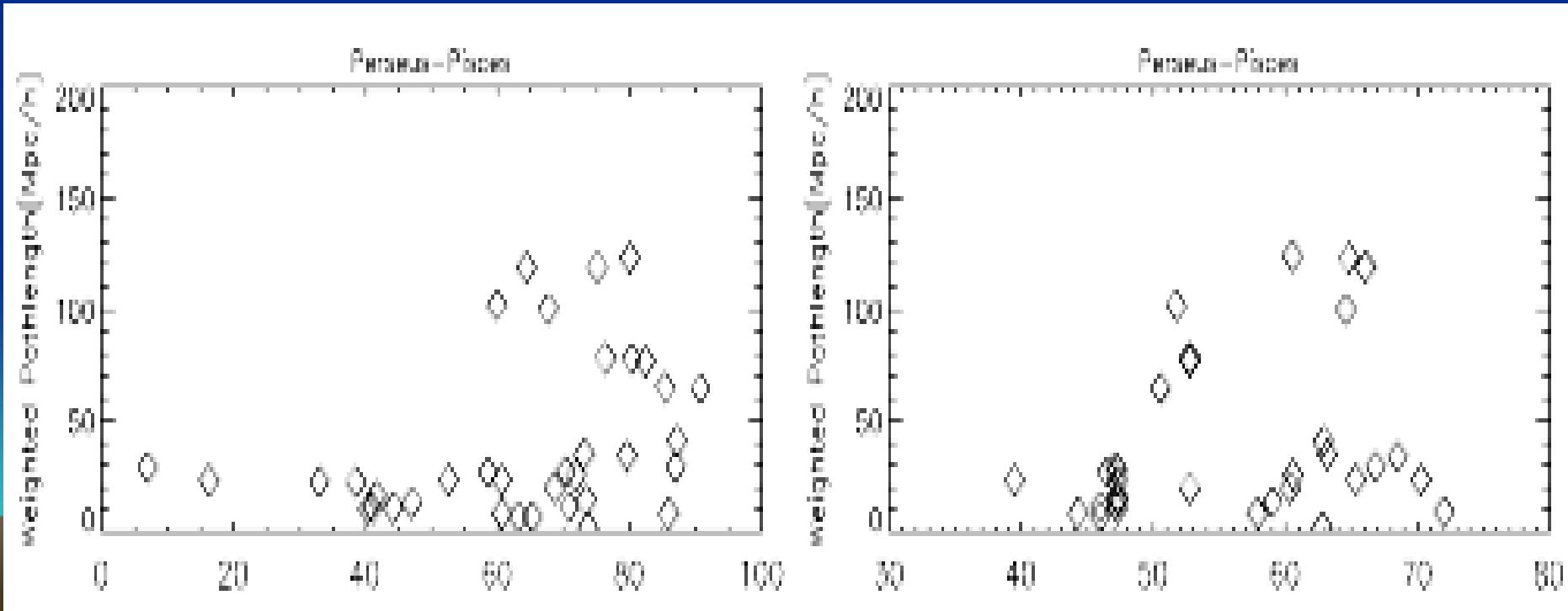
Galaxy column density vs RM
from 7° -smoothed data

(used the 2MASS galaxy survey)

Weighted path length vs RM

from 3-D Voronoi-tessilated IGM filament volumes
(\because 3-D spectroscopic z 's known).
also from 7° -smoothed data

(Used the CfA2 galaxy survey)



2 methods of IGM B analysis for the Perseus-Pisces supercluster

Results of RM + optical galaxy survey data(CfA2, 2MASS)

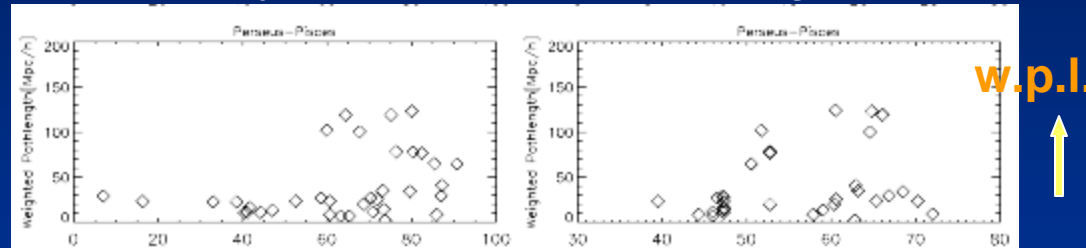
Xu et al. ApJ 2006

For the Perseus-Pisces supercluster:

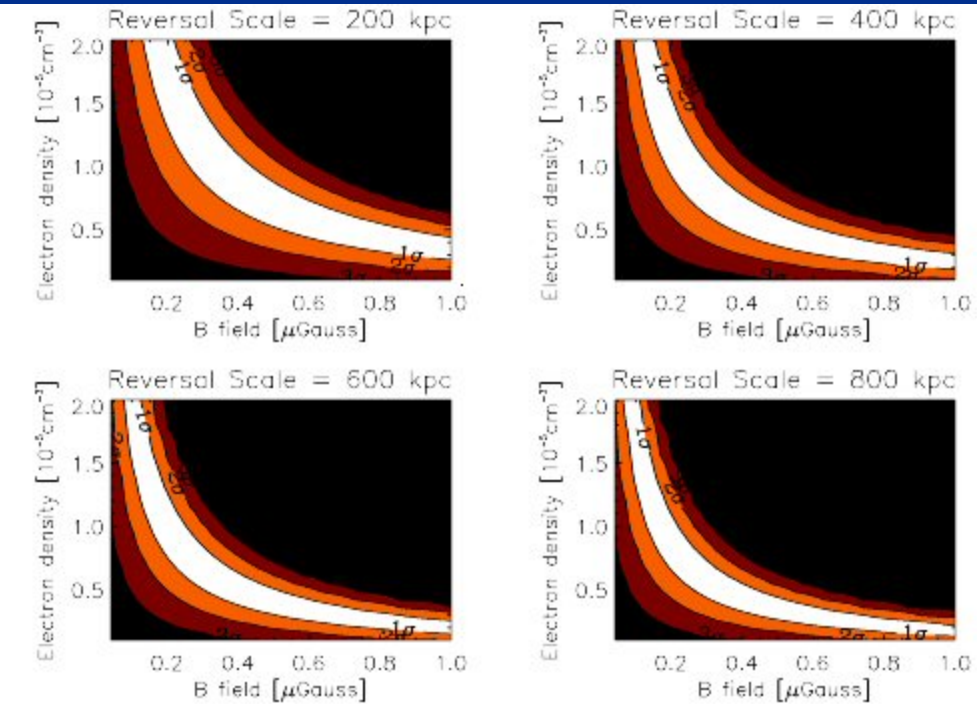
HEALpix algorithm
Col. density **2MASS**

Weighted path /.
Voronoi diagrams. **CfA2**

2 independ. measures of
pathlength through the
intergalactic filament



RM →



Result : $\langle \mathbf{B} \rangle_{\text{IGM}} \approx 10^{-7} \text{G}$
within the Perseus-Pisces
IGM ``filament''

The *Xu et al. 2006* (RM)- (2MASS/CfA) results of $\sim 10^{-7}$ G
are roughly consistent with:

1. Calculated, space –averaged, supermassive ($\gtrsim 10^7 M_\odot$)BH magnetic energy ($B^2/8\pi \times Vol.$) output (shown above)
2. Models/Predictions of LSS filament fields amplified by LSS gravitational infall.

(*H.Kang, D.Ryu & P.L.Biermann ApJ 335, 19, 1998 + others since.*

Most recent: *J. Cho & D.Ryu, ApJL, 705, 90, 2009*
predict:

$$\sigma_{RM} \sim 15 \left(\frac{n_e}{10^{-4} \text{cm}^{-3}} \right) \left(\frac{\langle |B| \rangle}{3 \times 10^{-7} \text{G}} \right) \left(\frac{l}{300 \text{kpc}} \cdot \frac{L}{5 \text{Mpc}} \right)^{0.5} \text{rad m}^{-2}$$

3(c)

A recent B_{IG} probe, using synchrotron radiation

- Search for intergalactic, diffuse synchrotron radiation,
- Until recently, difficult to isolate from foreground Galactic diffuse emission
- New method combines world's largest single dish (Arecibo) telescope with the precision imaging DRAO Interferometer.
- Searched in part of the Coma supercluster (100Mpc away), near the Galactic pole



0.4 GHz extragalactic diffuse synchrotron emission

P.P. Kronberg (LANL/Toronto), R. Kooches (DRAO), C.J. Salter, P. Perillat (Arecibo)
ApJ 659, 257, 2007

Arecibo 305m Telescope, PR



*2 mm rms optics
illuminated area $\approx 225\text{m}^2$
uv overlap with DRAO $\approx 200\text{m}$*

Dominion Radio Astrophysical Observatory

Penticton BC, Canada

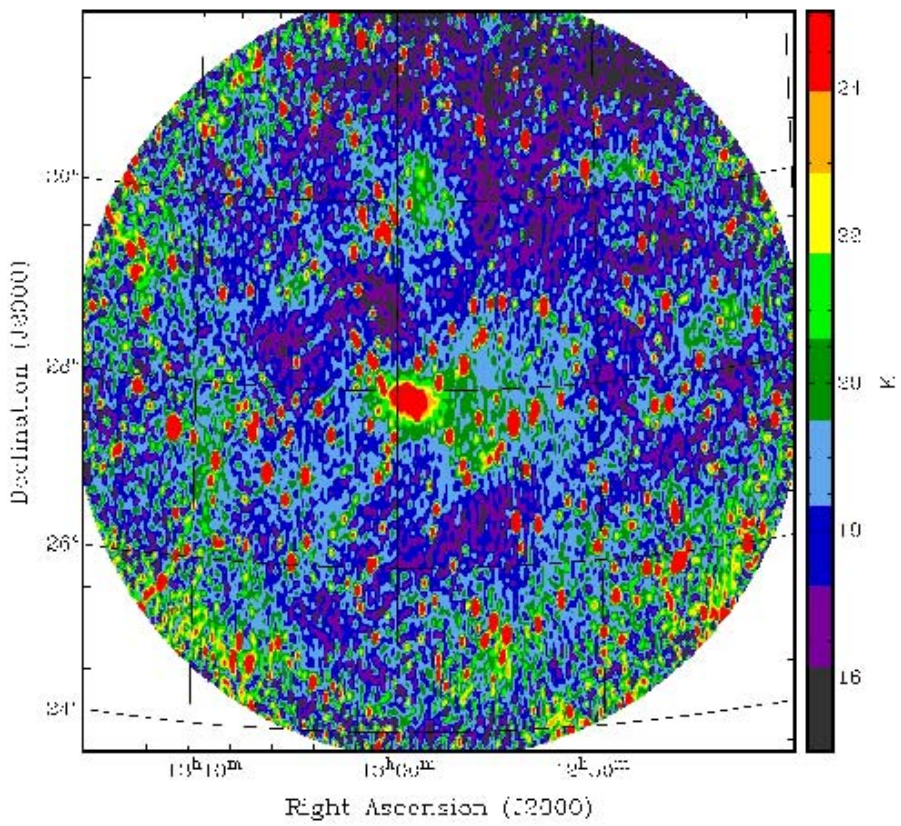


Max. separation = 617m

Min. projected separation \approx 18m

In 12 days, 1 full image within 9° circle at 408 MHz

8° dia. Field containing combined Arecibo + DRAO data, at a resolution of 2.5' x 6.5' 0.4 GHz

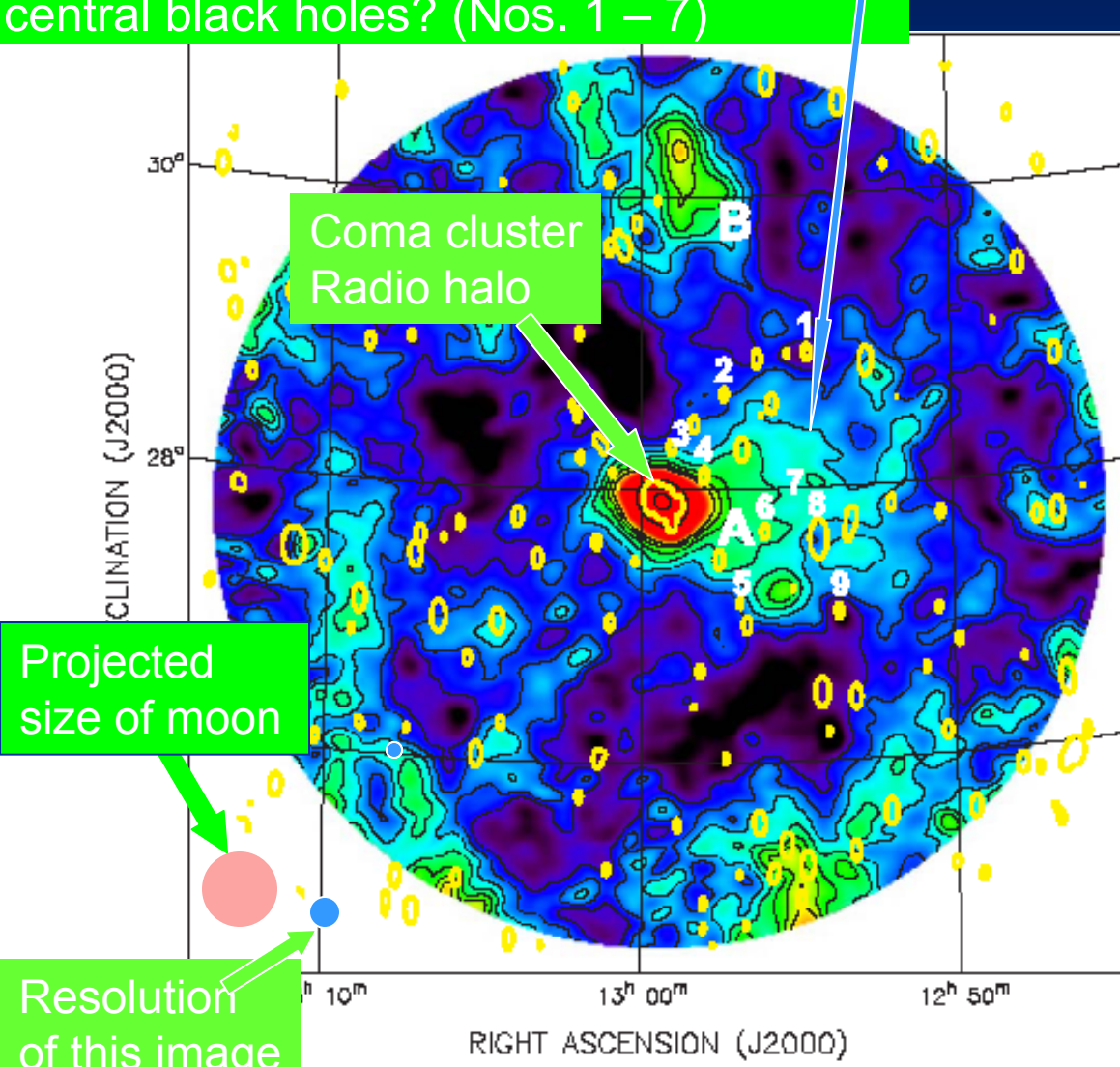


2.7K CMB background and galactic foregrounds ($\approx 18\text{K}$) are included

COMBINED Arecibo-DRAO image, smoothed to 10' (Arecibo) resolution

P. Kronberg, R. Kothes, C. Salter, & P. Perillat ApJ 659, 267, 2007

Collective energization of several galactic central black holes? (Nos. 1 – 7)



REMOVED:

- Discrete sources
- CMB + linear plane Milky Way foreground

Strongest discrete sources re-overlaid as yellow ellipses

- Black contours at 1.4, 1.9, 2.4, 2.9, 3.4, 3.9, 4.4, 10, 40K
- $\sigma \approx 250\text{mK}$ at 430 MHz

Region A (2 – 3 Mpc in extent) requires a distributed “fresh” energy source – plausibly provided by the ~ 7 embedded, radio galaxies.

RESULT:

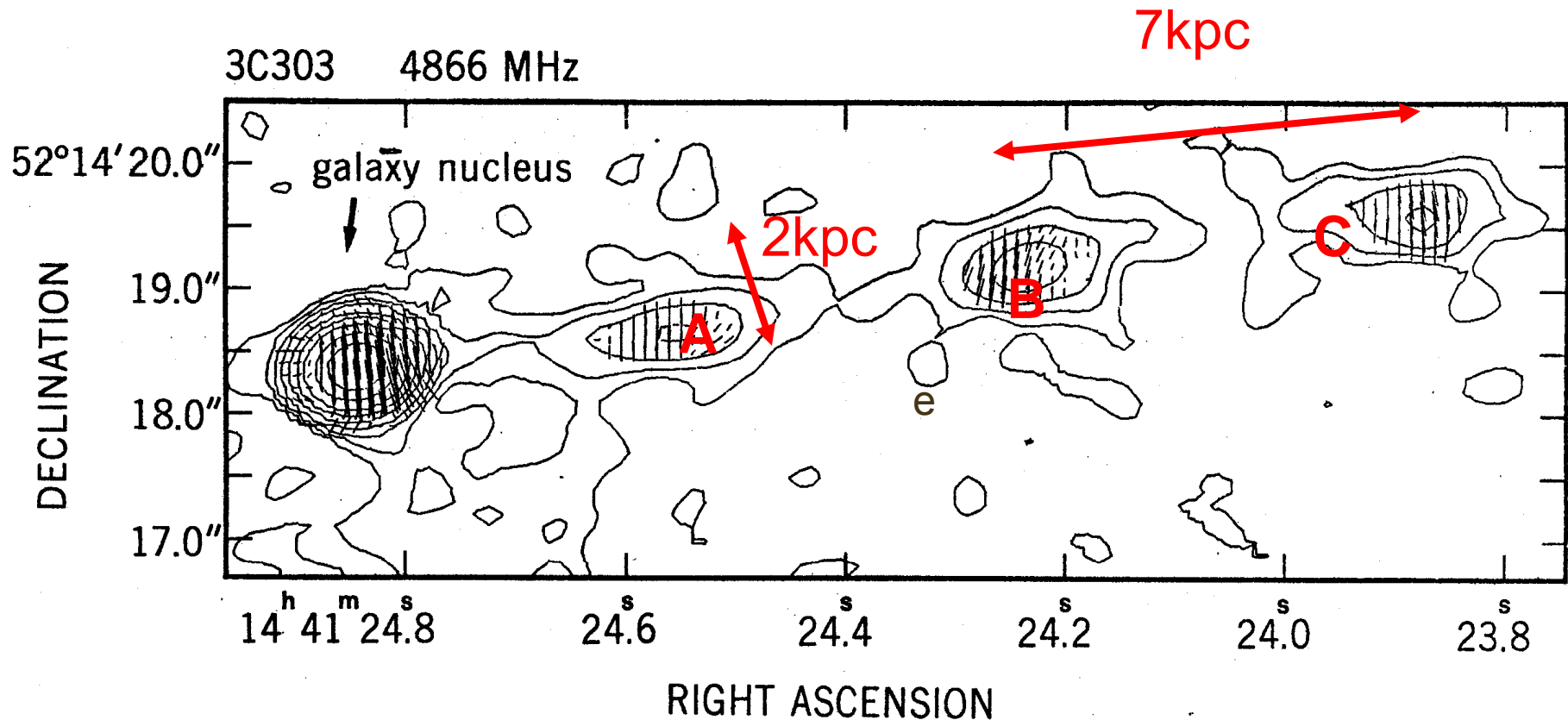
$$\langle |B| \rangle \approx 10^{-7}\text{G} \text{ over 2 – 3 Mpc}$$

4

Possible UHECR acceleration sites in jets and lobes

- Nearby candidate: Cen A
- Diagnosable “test” jet: 3C303 at $z = 0.14$

Jets as UHECR accelerators?

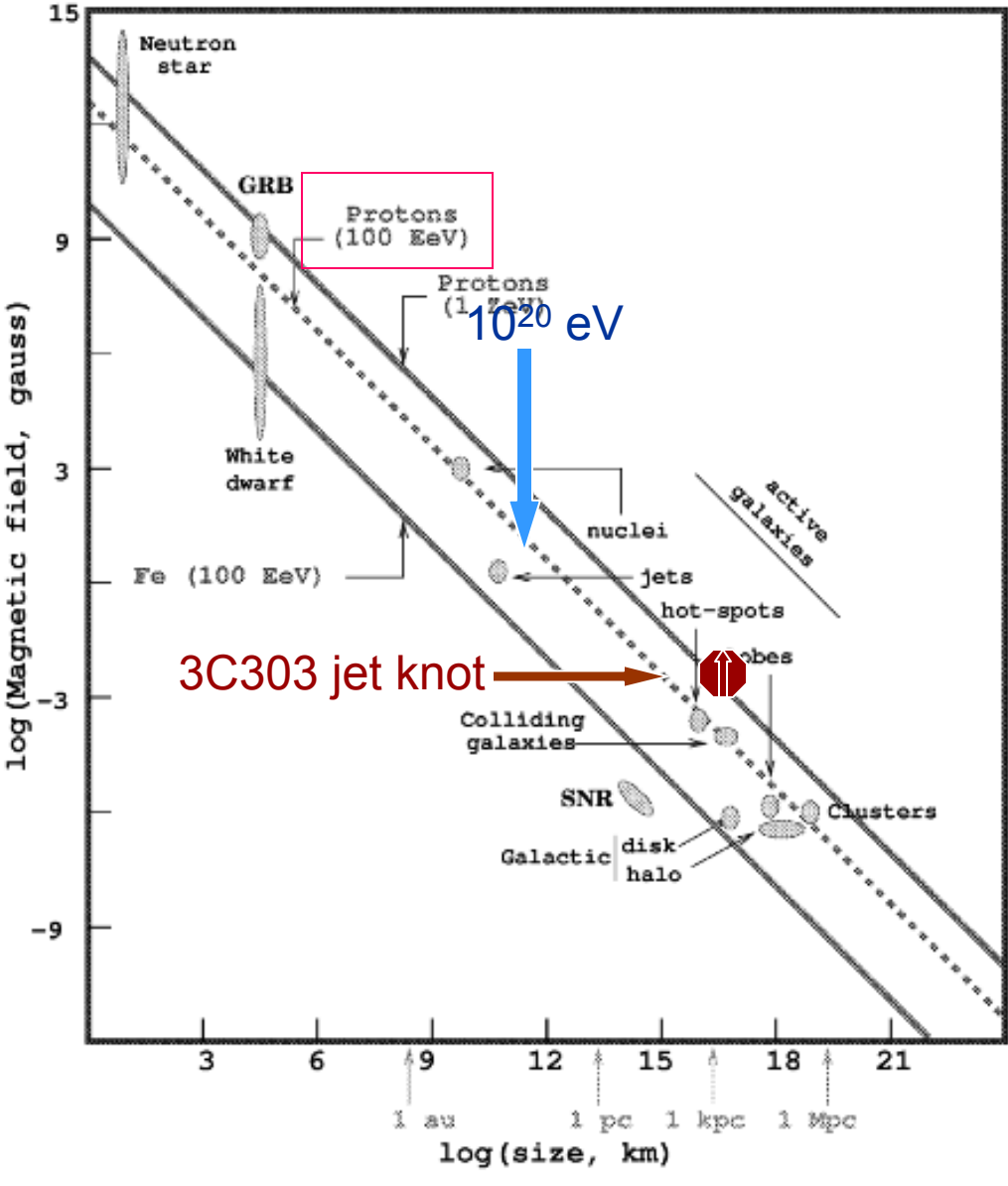


$$E = \frac{B}{3 \text{ mG}} \times \frac{L}{1 \text{ kpc}} \Rightarrow 10^{19} \text{ eV}$$

Plasma parameters in the 3C303 jet

- Given B and n_{th} measured in the 3C303 jet, (and scaling to $T=10^8\text{K}$)
- Plasma $\beta = \frac{n k T}{B^2 / 8\pi} \approx 10^{-5} T_8$, confirms very little thermal plasma
- $|B| \sim 3 \text{ mG}$ in the (synch. radiating) jet knots,
over $\sim 1\text{kpc}$
- Consistent with a magnetically confined, Poynting flux-dominated jet.

Lapenta & Kronberg ApJ 2005



Hillas plot (A.M. Hillas *ARA&A* 1984)
 (adapted from **M Ostrowski**
astro-ph/0101053)

Conditions required for acceleration to an energy above the required Line.

3C303's knot parameters make them potential acceleration sites for CR nuclei up to $\sim 10^{19-20}$ eV

Transverse RM gradient in the jet

- For knot “C”, the RM image of 3C303 enables a measurement of the transverse ∇RM (radians/m⁻²/m) over a knot. i.e. ∇RM is perpendicular to the jet!
- B (RM) reverses sign on the jet axis. $|B| \approx 3\text{mG}$ estimated from measured synchrotron emissivity ($\gtrsim 1\text{mG}$)
- a galaxy-scale, current-carrying “wire”
- result for 3C303: $I = 7.5 \times 10^{17} (B_{-3}^G)$ [r= 0.5kpc] ampères
- I is directed AWAY from the galaxy AGN nucleus in this knot
- Intrinsic knot polarization consistent with low- ϕ jet helical field

*Reported in H. Ji, P.P. Kronberg, S.C. Prager, D. Uzdensky,
Physics of Plasmas **15**, 058302-8, 2008*



5

Magnetism in the widespread IGM to the largest measurable redshifts

1. Optimally remove the galactic foreground
 $RM \rightarrow$ evaluate residual RM (RRM)
2. Test for $\sigma^2(RRM)$ vs. z



RM search at high z for a widespread B_{IGM}

- Began in 1970's

*M. Rees, M. Reinhardt, P. Kronberg
M. Simard-Normandin, A. Nelson,
J.P. Vallée*

- Why was it of interest?
 - Then Ω_B was $\simeq 1$,
 $\therefore n_e(z)$ is high enough to
“illuminate” $B_{\text{IG}}^{} \text{ to high } z$!
 - Now, $\Omega_B \simeq 0.04$; too little
to detect an RM_{IGM}
BUT
 - high energy extragalactic events
can probe/limit $|B|$ to
 ~ 10 orders of magnitude fainter.

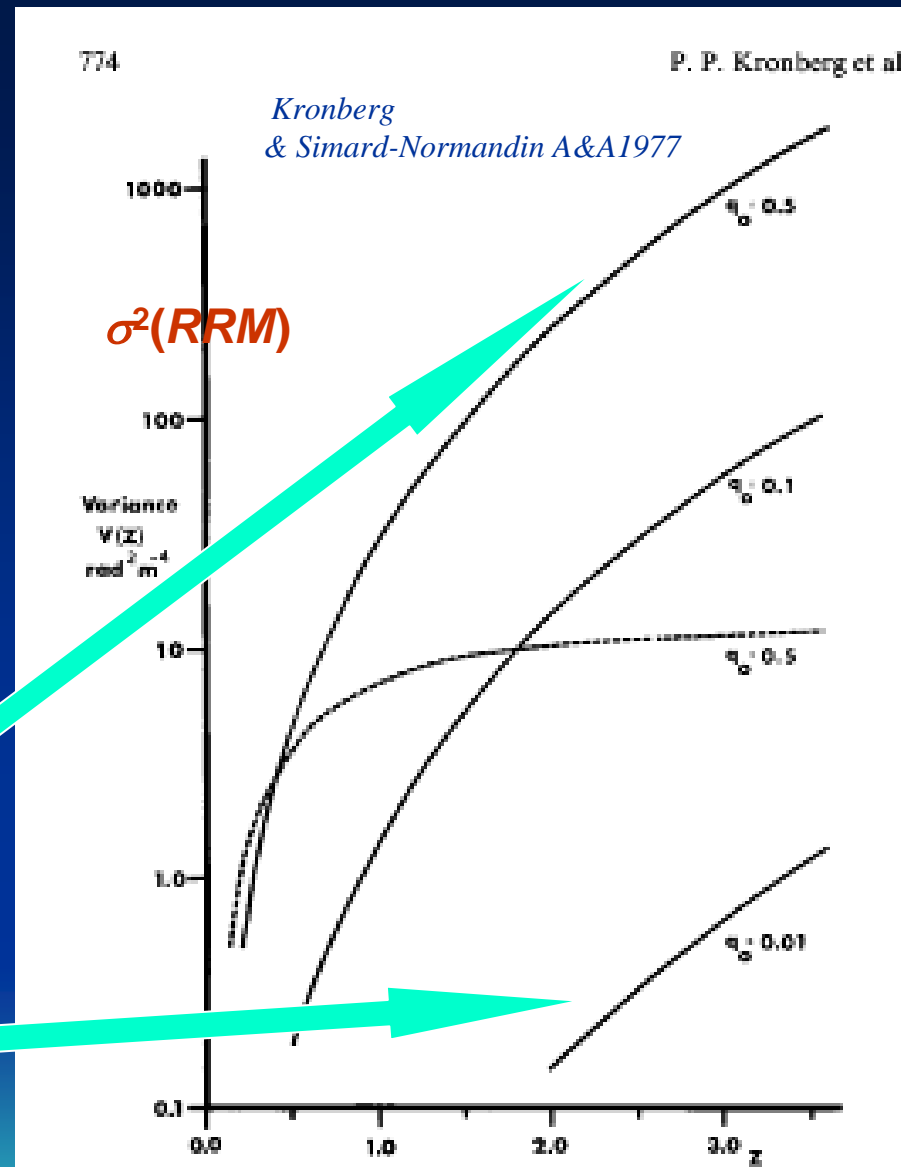


Fig. 1. The calculated variation of $V(z)$ for models 1 (solid lines) and 2 (dashed line) over the redshift range $0 < z < 3.6$. The following values were assumed: $B_0 = 1.8 \cdot 10^{-8}$ Gauss, $\eta = 1$, $H_0 = 75 \text{ km s}^{-1} \text{ Mpc}^{-1}$, $t_0 = 1 \text{ Mpc}$, and $f = 1/64$ for model 2. Model 1 is shown for q_0 ($= \Omega/2$) values of 0.5, 0.1 and 0.01

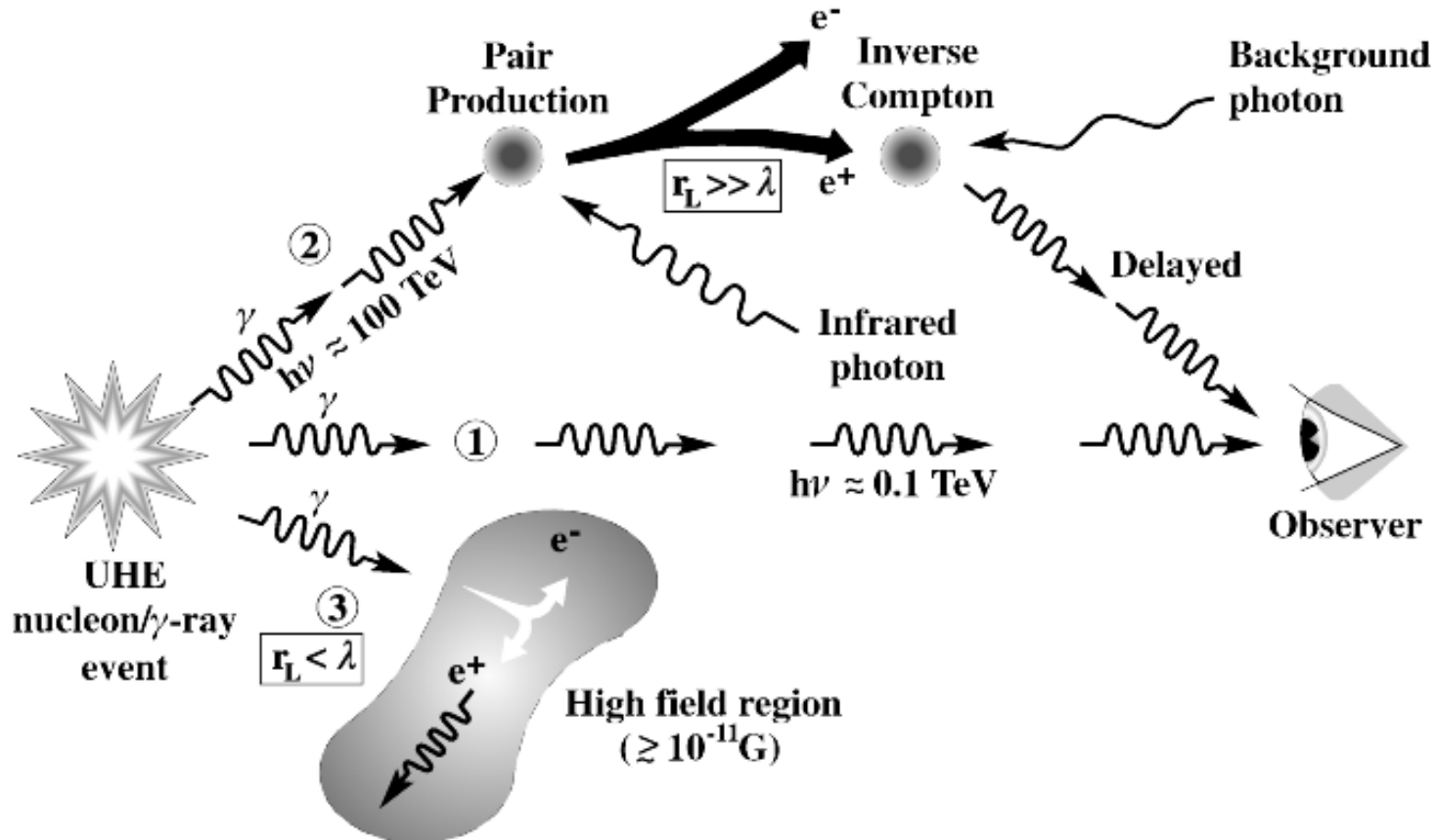
Magnetic fields in cosmic voids? from where? how to detect them?

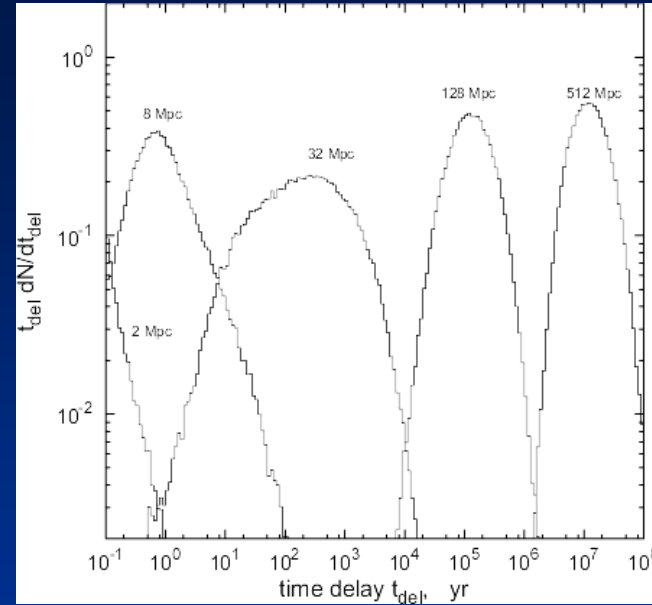
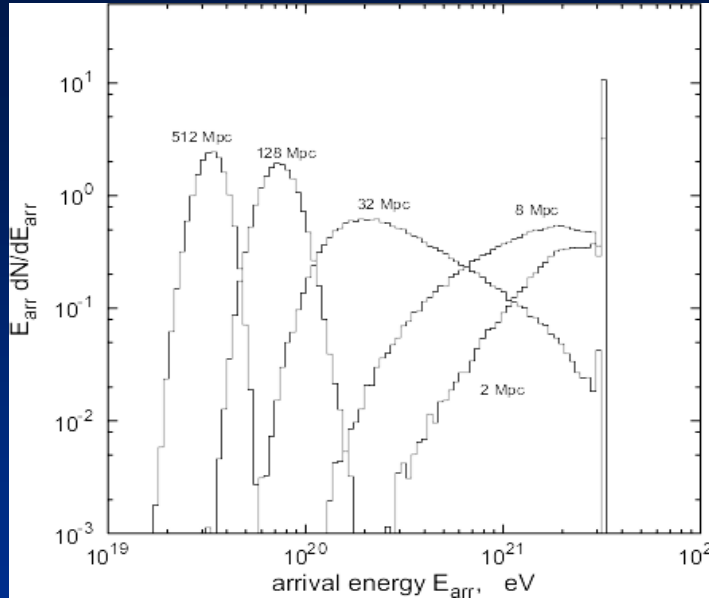
- Diffusion out of the walls and filaments? (galaxy-supplied)
- Relic of a pre-galactic, or primordial field?
- B measurements still mainly *Gedanken-Experimente*,
- Most involve high energy particle & photon propagation
- Time of arrival, deflection, energy and composition

At $E \gtrapprox 10^{18}$ eV, all of ``empty'' i.g. space
becomes a (passive) particle physics laboratory!!

Energy cascade cartoon of a broadband γ -ray burst could probe a very weak IGM field

High energy $h\nu - e^+e^-$ cascades in the intergalactic medium





*Stanev T., Engel, R., Mücke, A., Protheroe, R. J., Rachen, J. Phys Rev. D, **62**, 0930052000*

(left)

The received CR energy distribution on Earth for a monoenergetically injected proton energy of $10^{21.5}$ eV for a randomly orientated

$B_{IG} = 10^{-9}$ G at progressively larger distances, up to 512 Mpc. The energy is reduced by the GZK effect (most severe), B-H pair production losses, and adiabatic losses.

(right)

The relative time delay for protons injected at the same distance when propagated through a randomly oriented magnetic field of 10^{-9} G, where $I_0 = 1$ Mpc.

Discrete magnetized *intervenors* in the universe

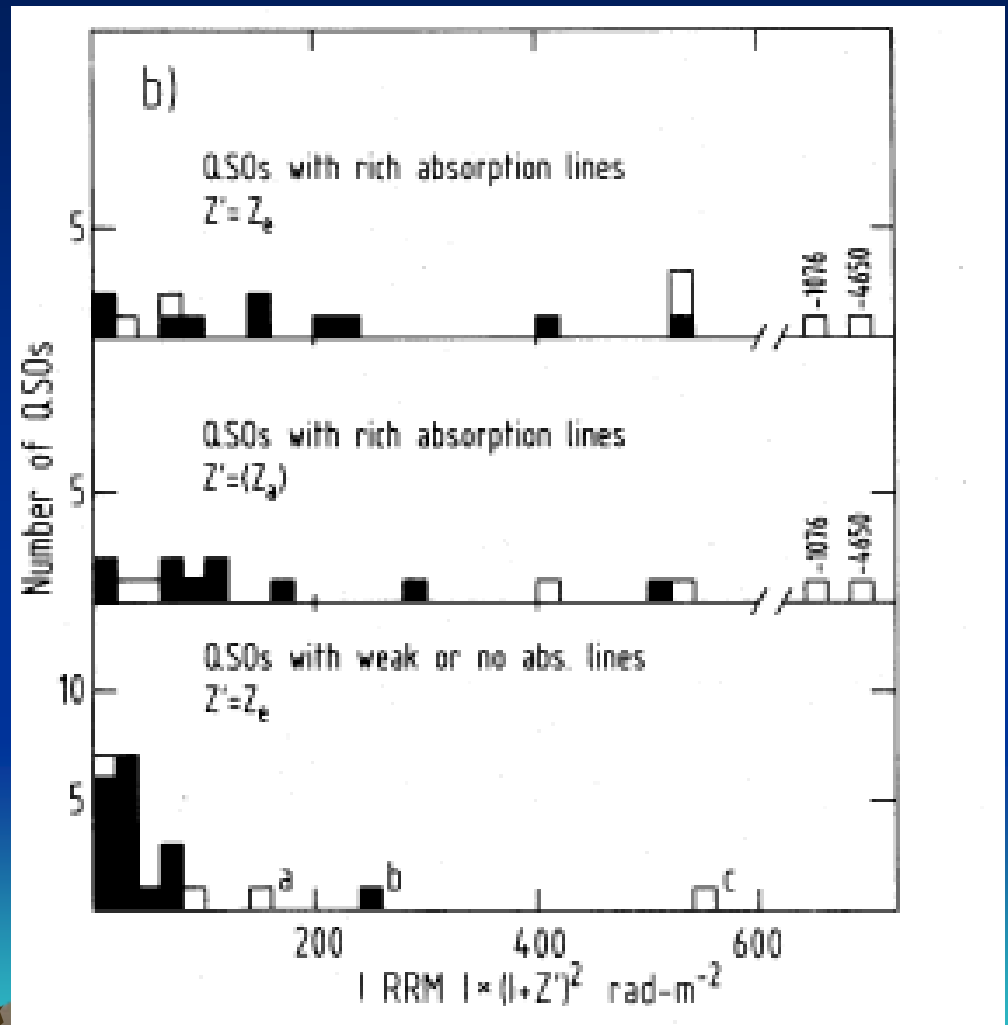
Note: galaxy clusters barely count here!
 $\rightarrow \rho(z) \cdot \sigma(z)$ is too small relative to
that of galaxies



Detections of magnetized optical absorption line systems

G.L. Welter, J.J. Perry, & P.P. Kronberg
ApJ 279, 19, 1984
(119 RM sample, 40 had spectra with
strong optical absorption lines)

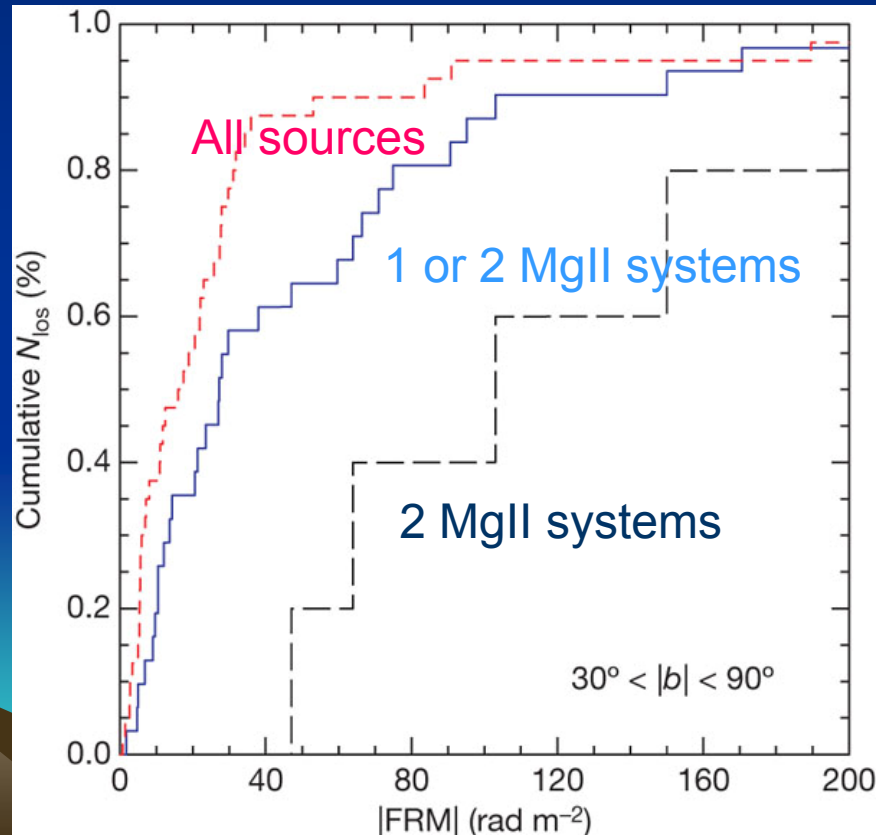
P.P.Kronberg & J.J. Perry,
ApJ 263, 518, 1982
(37 RM + Abs. spectrum QSO's)



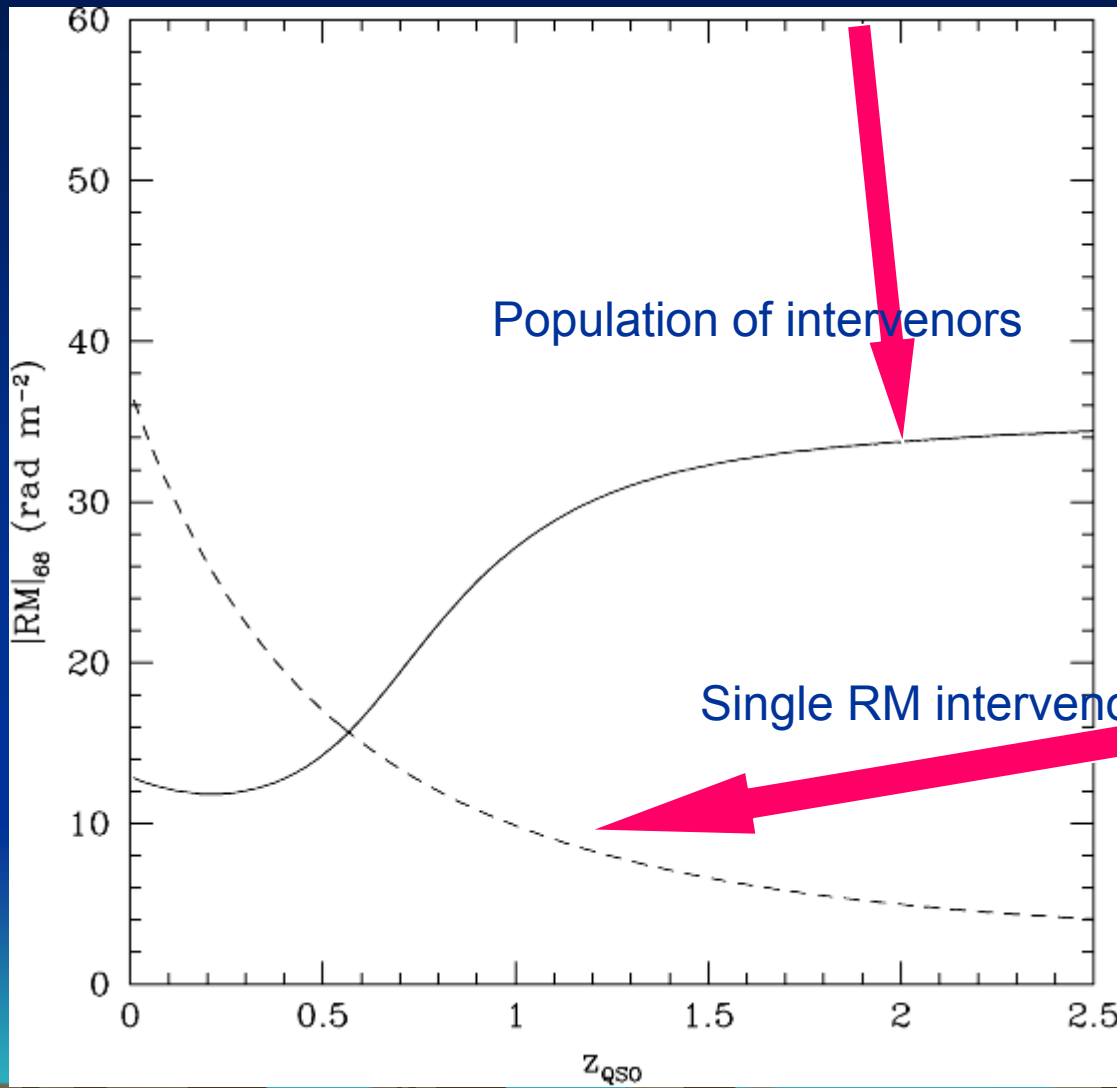
Cumulative plots of RM for 3 different MgII absorption line groups

M.L. Bernet, F. Miniati, S.J. Lilly, P.P. Kronberg, M. Dessauges-Zavadsky Nature 454, 302-4, 2008

Method: G.L. Welter, J.J. Perry & P.P. Kronberg ApJ 279, 19, 1984



Observed RM increase through a population of intrinsically similar Faraday intervenors (galaxy systems) out to $z = 2.5$



$\Sigma (RM_i)$ for a population of discrete magnetized L^* galaxy intervenors

RM_0 of a 37 rad m $^{-2}$ intrinsic Faraday rotation at z_{QSO}

--illustrates $(1 + z)^{-2}$ decrease of RM with z

N(RRM, z) is a complex, multivariate distribution!

It contains:

- a strong $(1+z)^{-2}$ factor ($0.06 \times RRM_0$ at $z = 3$!)
- varying fraction of real RRM< “outliers”
- RM outliers have different causes
- multiple populations of galaxy and halo intervenors
- galaxy groups and (fewer) galaxy clusters
- small subset of high intrinsic (& evolving?) RM’s
- Cross-section evolution
- etc.

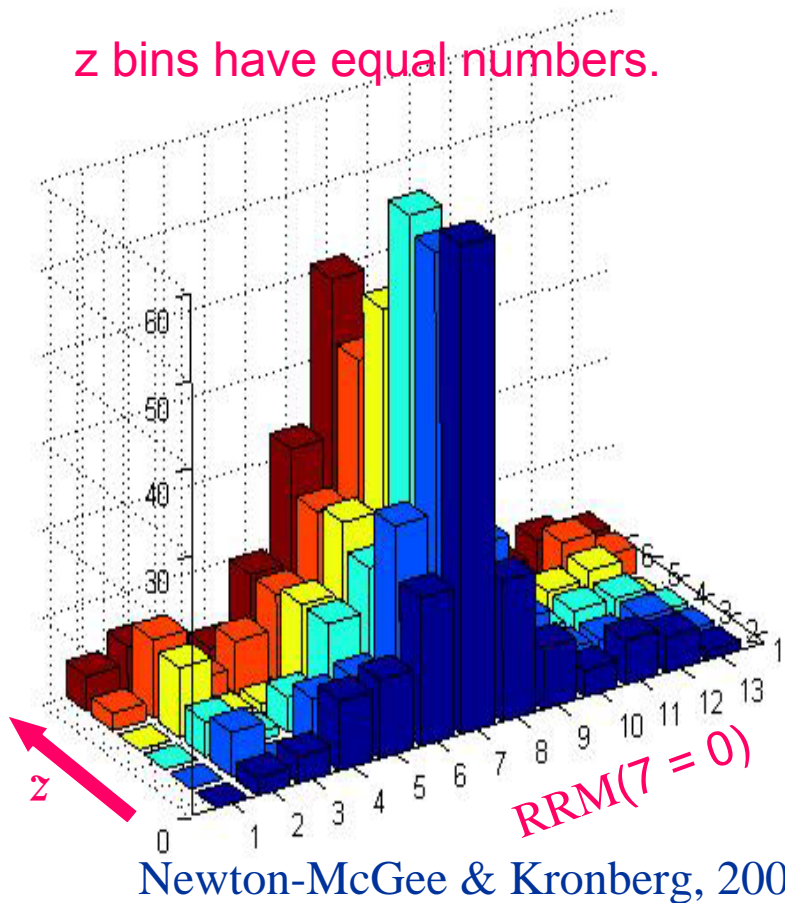
Philipp Kronberg



Galaxy-corrected ``residual'' RM (RRM) for ~ 800 RM sources to $z \approx 3.4$

Katherine Newton-McGee and Philipp Kronberg 2009

z bins have equal numbers.



1. smallest RRM bin declines with z , then reappears as $z \rightarrow 3$
2. strongest RRM perturbations are at $\approx 20 - 100$ rad m $^{-2}$

For a typical intervening
``galaxy system'' at $z = 2.5$:; and
adopting optical dN/dz statistics
(N_e = ionized H column)

$$\langle B_{||} \rangle \geq 5.5 \times 10^{-7} G \left(\frac{1+z_c}{3.5} \right)^2 \times \left(\frac{\sigma_{RRM}}{20 \text{ rad m}^{-2}} \right) \times \left(\frac{N_e}{1.7 \times 10^{21} \text{ cm}^{-2}} \right)$$

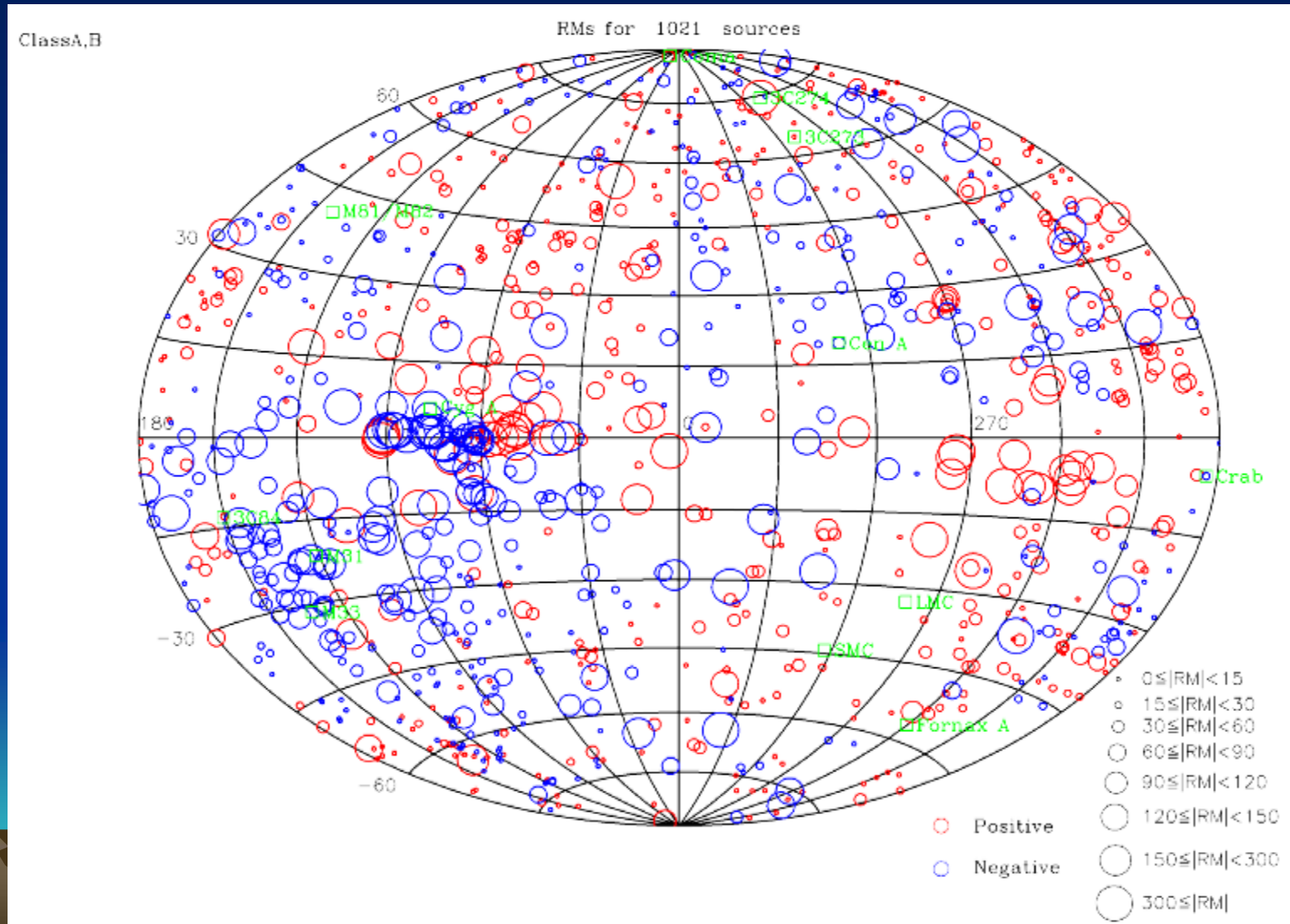
Principal new result: The Universe begins to get “Faraday RM – opaque” at ~ 1.4 GHz to sources beyond $z \sim 2.5$

* * *



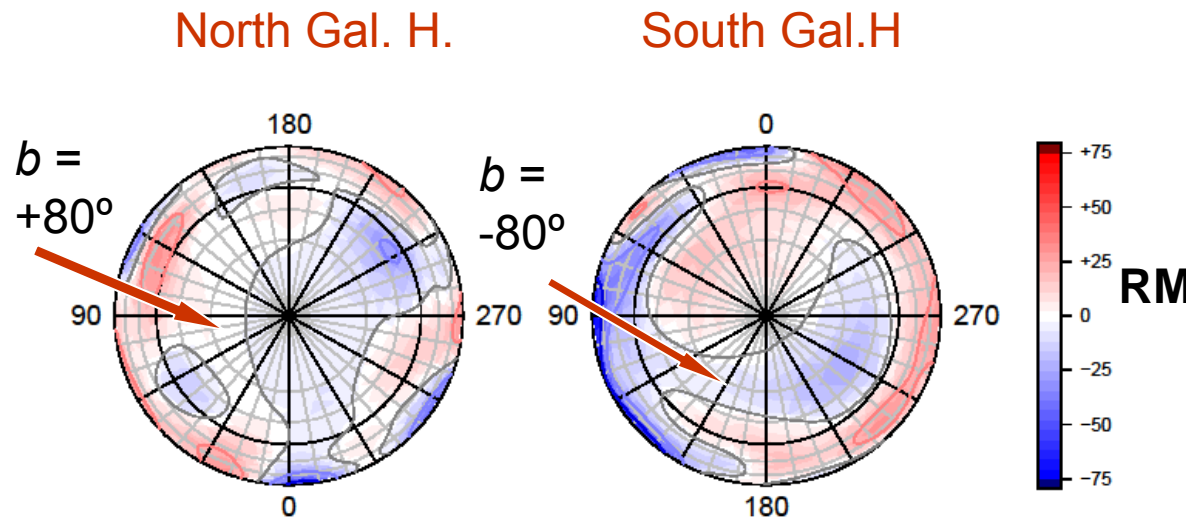
Faraday rotations of extragalactic radio galaxies and quasars

Including the RM “outliers” --to be “filtered out” data:epoch ~1995



Bayesian smoothed RM's in the Galactic caps $|b|>30^\circ$

M.B. Short, D.M. Higdon & P.P. Kronberg
Bayesian Analysis 2, 665, 2007



Better data and more refined analysis are underway